III.1
$^{87}Sr/^{86}Sr$ ratios discrimination applied to the Palaeozoic carbonates of the Ossa-Morena Zone

Index

III.1.1. Introduction

The definition of lithostratigraphic successions in metamorphic and strongly deformed domains is essential to constrain its geodynamical evolution. However, in these cases, the paleontological data are often scarce and the chronological establishment of a local lithostratigraphic succession is dependent of the correlation with well-defined lithostratigraphic successions with fossiliferous data or, in some cases, using the geochronological data to constrain the age of the lithostratigraphic successions.

In Abrantes, despite the greenschist-amphibolite metamorphic recrystallization and the strong variscan deformation (Romão et al., 2010; Moreira, 2012; Moreira et al., 2015), structural and petrological data show a lithostratigraphic succession similar to the Neoproterozoic-Cambrian series of Ossa-Morena Zone (OMZ; e.g. Oliveira et al., 1991; Gozalo et al., 2003). One of the Abrantes lithostratigraphic units is a carbonated succession (S. Miguel do Rio Torto

Carbonates), mainly composed of dolomite and calcite marbles interbedded with mafic volcanic rocks and calc-schists (Moreira et al., 2015). The litostratigraphic and petrographic features of this unit are similar to the Lower Cambrian carbonated successions of OMZ (Oliveira et al., 1991; Gozalo et al., 2003; Araújo et al., 2013). Nevertheless, not only the carbonate sedimentation in OMZ is not exclusive of Lower Cambrian, but often its age is highly debatable in some sectors, as in Estremoz Anticline and in Ficalho (Piçarra, 2000; Piçarra and Sarmiento, 2006; Pereira et al., 2012).

The determination of the $^{87}Sr/^{86}Sr$ of the OMZ carbonates could help to constrain the lithostratigraphic correlations between them. Indeed, by comparing the $^{87}Sr/^{86}Sr$ ratios in marbles and limestones from different domains of OMZ, with available chronological and isotopic data, it is possible to establish strontium isotopic signatures for the Cambrian and Devonian carbonated episodes. This methodology allows a coherent correlation between OMZ carbonates.

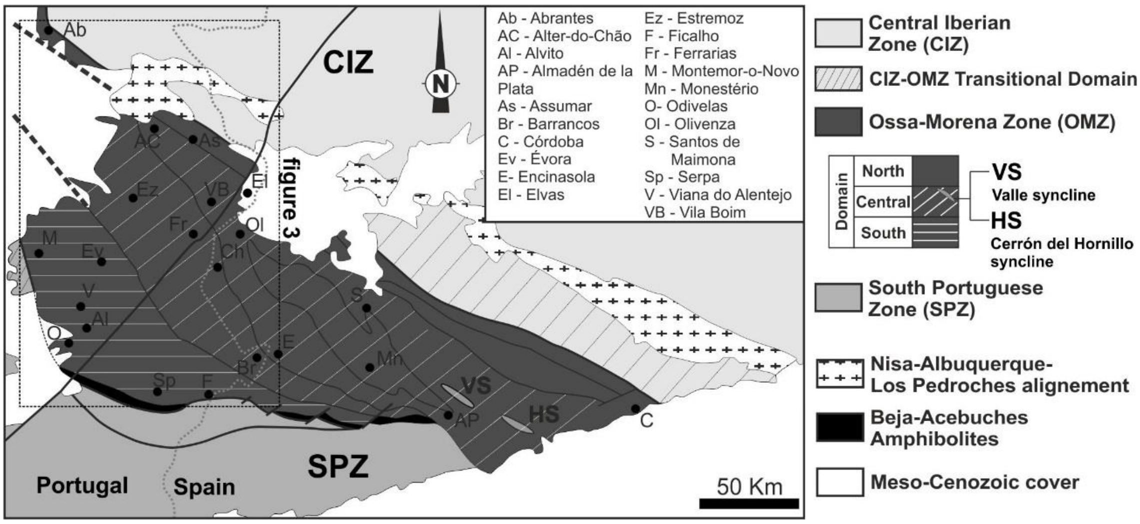

Figure 1 – Geological sketch of the OMZ in the context of neighboring tectonostratigraphic Variscan Zones text (adapted from Oliveira et al., 1991 and Robardet and Gutierrez-Marco, 2004).

III.1.2. The Ossa-Morena Zone Carbonates

The stratigraphic successions defined for OMZ show the presence of four regional distinct carbonate sedimentation episodes:

(i) The first episode, Cambrian in age (Ovetian-Marianian – Cambrian Stage 2; Oliveira et al., 1991; Gozalo et al., 2003, Alvaro et al., 2014), is related with the first pulses of Variscan Cycle during the continental rifting process (Sánchez-Gárcia et al., 2008; 2010; Moreira et al., 2014a). This episode is characterized by sequences of dolomite and calcite marbles or limestones, sometimes with siliciclastic beds and interbedded metavolcanic rocks (Oliveira et al., 1991; Vera, 2004; Sánchez-Gárcia et al., 2008; 2010; Pereira et al., 2012; Araújo et al., 2013; Moreira et al., 2014a). The Ovetian-Marianian age is constrained by paleontological data in Spain (Gozalo et al., 2003; Vera, 2004 and included references) and in Portugal (Alter-do-Chão-Elvas Domain; Oliveira et al., 1991; Araújo et al., 2013). In the successions with no biostratigraphic data, the age is based on lithostratigraphic correlations, such as in the Abrantes, Estremoz, Ficalho and Viana do Alentejo successions (Fig 1; Oliveira et al., 1991; Moreira et al., 2015; 2016);

(ii) An Upper Ordovician episode (Kralodvorian – Ka3 and Ka4; Robardet and Gutierez-Marco, 2004; Sarmiento et al., 2008; 2011), the Pelmatozoan Limestone, is preserved in Valle and Cerrón del Hornillo synclines (Fig. 1; Robardet and Gutierrez-Marco, 1990; 2004; Sarmiento et al., 2008; 2011). This unit is characterized by massive limestones, sometimes bioclastic (Sarmiento et al., 2008; 2011), with evidences of dolomitization. The massive features are less evident on top and bottom of the sequence, where laminated textures were developed. On top of the limestones succession, karstified morphology was described (Robardet and Gutierez-Marco, 2004).

(iii) Also in Valle and Cerrón del Hornillo synclines, the Scyphocrinites Limestone has an Upper Silurian age, with the bottom of sequence could be Late Ludlow or early Pridoli (Robardet and Gutierez-Marco, 1990; 2004). This unit consists in dark limestones interbedded with calcareous shales. These limestones are not represented in Silurian succession of Barrancos area (temporally similar to Xistos Raiados Formation; Piçarra, 2000). Although, in Murtiga Formation (Encinasola area), considered equivalent of the Xistos Raiados Formation, Pridoli limestones have been mentioned (Robardet and Gutierez-Marco, 2004).

(iv) The fourth episode is Lower-Middle Devonian in age, being represented in the SW domains of the OMZ (Machado et al., 2009; 2010; Moreira et al., 2010; Moreira and Machado, in press). Machado et al. (2009; 2010) described a calciturbiditic sequence (Odivelas Limestone), recently interpreted as a reef system (Moreira and Machado, in press), spatially associated to basaltic rocks with low-K tholeiitic to calc-alkaline geochemical signatures (Rebolado Basalts; Santos et al., 1990; 2013; Silva et al., 2011). The paleontological data from the Odivelas limestones provides Emsian to Givetian ages (Conde and Andrade, 1974; Oliveira et al., 1991; Machado et al., 2009; 2010). Similar facies and ages (Eifelian to Frasnian) are also described in limestones associated to the Toca da Moura and Cabrela Carboniferous basins (Pena and

Pedreira de Engenharia Limestones near Montemor-o-Novo; Boogard, 1972; 1983; Machado and Hladil, 2010). These limestones are interpreted, at least in part, as Devonian olistoliths within the previous mentioned basins (Pereira and Oliveira, 2003; Pereira et al., 2006; Oliveira et al., 2013).

In addition, in some Carboniferous basins located in the Central and North domains of the OMZ (Robardet and Gutierez-Marco, 1990; Palácios Gonzalez et al., 1990; Medina-Varea et al., 2005; Armendáriz, 2006), some limestones are also described interbedded in siliciclastic sequences, however some of these limestones are not marine limestones.

Although the age of the Palaeozoic carbonated sedimentation in OMZ is usually well constrained, in the Estremoz-Barrancos sector and in Ficalho succession it is a highly debatable subject (Oliveira et al., 1991; Piçarra, 2000; Pereira et al., 2012; Araújo et al., 2013 and references therein). In these cases, overlying the basal carbonated unit (mostly dolomitic marbles – the Dolomitic Formation), a volcano-sedimentary complex with abundant calcite marbles is found (Oliveira et al., 1991; Araújo et al., 2013). The presence of crinoid fragments and conodonts in the calcite limestones of Ferrarias (which according to Piçarra, 2000 is equivalent of the neighbouring Estremoz Marbles), Barrancos and Ficalho, assigning at least an Upper Silurian to Devonian age to these limestones (Piçarra and Le Menn, 1994; Sarmiento et al., 2000; Piçarra and Sarmiento, 2006). These fossiliferous limestones are contained in the volcano-sedimentary complexes developed over the basal Cambrian Carbonated Units (Piçarra, 2000).

However, some authors argue that these ages could not be considered the depositional ages of the limestones, but results from mixing younger materials due to sub-aerial exposure and remobilization of faunal material (Pereira et al., 2012). The same authors obtain a 499.4 ± 3.3 Ma age (SHRIMP U-Pb zircon) in meta-rhyolites, that they considered intercalated into marbles from the Estremoz sequence, proposing a Middle-Upper Cambrian transition age for the Estremoz volcano-sedimentary complex. Nevertheless, field relations of these meta-rhyolites (Coelho and Gonçalves, 1970; Gonçalves, 1972) precludes such conclusion (see chapter V.2 for a discussion).

III.1.3. The $^{87}Sr/^{86}Sr$ Ratio Approach

As the isotopic ratio $^{87}Sr/^{86}Sr$ of oceanic waters has varied over the time (Fig. 2), its determination could be used in the correlation and, in some cases, dating the marine carbonates that preserve the seawater $^{87}Sr/^{86}Sr$ fingerprint (Burke et al., 1982; Veizer, 1989; Veizer et al., 1999; McArthur et al., 2012 and included references).

The $^{87}Sr/^{86}Sr$ variation has been due by changing the fluxes of Sr to the ocean, from the two main sources: mantle and continental crust (McArthur, 1994; Veizer et al., 1999). In middle ocean ridges, the hydrothermal circulation induces the interaction between oceanic crust and seawater, generates a modification of strontium isotopic ratio in seawater: the loss of Sr from seawater is replaced by leached Sr from middle ocean ridge rocks, decreasing the $^{87}Sr/^{86}Sr$ of marine seawater (McArthur, 1994). On the other hand, the continental weathering supplies are higher than that of marine Sr. Indeed, addition of continental crust Sr to the ocean, therefore increases the marine $^{87}Sr/^{86}Sr$ ratio (McArthur, 1994). Nowadays, the $^{87}Sr/^{86}Sr$ ratio in seawater is always higher than 0.703 (minimum value of mid ocean ridge rocks) and usually lower than 0.713 (best estimated value of modern rivers; McArthur, 1994).

The analytical precision of the $^{87}Sr/^{86}Sr$ ratio that can be measured is ± 0.00002 (McArthur, 1994). This precision makes analytically indistinguishable the ratio variation in seawater from worldwide localities. This uniformity is resulted from the residence time of Sr in the Ocean that is far longer than the time it takes currents to mix the oceans, so the oceans are thoroughly mixed on time scale that are short relative to the rates of gain and loss of Sr (McArthur, 1994; McArthur et al., 2012). As such, it is assumed that the ocean has always been well mixed, as in present, and consequently is isotopically uniform with respect to $^{87}Sr/^{86}Sr$. This fact allows to correlate and even date some marine rocks and minerals.

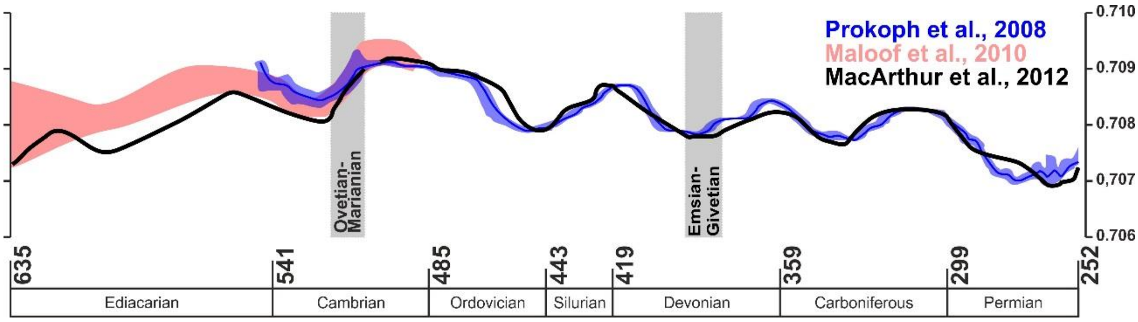

Figure 2 – Variation of $^{87}Sr/^{86}Sr$ through the Ediacarian and Palaeozoic times (curves adapted from Prokoph et al., 2008; Maloof et al., 2010; MacArthur et al., 2012).

III.1.4. Sample preparation and methods

37 samples of OMZ carbonate rocks were collected. After sample characterization by conventional petrographic techniques, they underwent specific preparation, such as cleaning and removing meteoric surface alteration followed by crushing, gridding and sieving, in order to obtain powdered carbonate samples smaller than 63 µm, enriched in carbonate specimens. The used methodology allow to concentrate the carbonated phases in powdered samples.

The detailed mineralogical composition of carbonates was analysed in a X-Ray difractometer (XRD – Bruker D8 Discover with DaVinci geometry) and using a Lynxeye linear detector (Hercules Laboratory, University of Évora). The scans was collected from 2θ 3º to 75º, with steps of 0.005º and one second by step. The semi quantification of the phases abundances were done using the DIFFRAC.SUITE software from Bruker by the RIR-Reference Intensity Ratio (Hubbard et al., 1976; 1988 and included references).

The strontium isotope analyses were done using a Mass Spectrometer Thermal Ionization (TIMS) with a VG Sector 54 spectrometer (Isotopic Geology Laboratory, University of Aveiro). The main procedure involve a first stage of rocks sample dissolution with HCl with some drops of HF and HNO_3 for the carbonates. Afterwards, the remaining solutions, including the carbonate leachated samples, were dried and re-dissolved in HCl and subject to a conventional two-stage ion chromatography separation with cation exchange resins for Sr purification. This methodology should guarantee the non-carbonate fraction separation from the whole sample. After the carbonate concentration and purification in each sample the isotopic measurements of $^{87}Sr/^{86}Sr$ ratios were performed by means of a thermal ionization mass spectrometry (VG Sector 54).

III.1.5. Geological framework, Petrography and XRD analysis of OMZ Carbonates

The 37 carbonate samples from the OMZ Paleozoic Carbonates were characterized by conventional petrographic techniques, with special attention to textural, mineralogical and metasomatic (i.e. secondary dolomitization) features and by XRD analyses. The samples includes marbles and limestones, with calcite and dolomite as the main mineral carbonate specimens, and one sandstone with calcite cement. Some dolomite carbonates show macro and microscopic textural evidences of secondary dolomitization, while in others the dolomitization is interpreted as “primary” and/or diagenetic.

A short general framework for the collected samples and the main petrographic features of analysed samples are summarized below according to the geographic sectors of samples provenience.

III.1.5.1. Northern OMZ Carbonates (Abrantes, Assumar)

From the northern OMZ domains, 7 samples were collected, 6 from Abrantes and 1 from Assumar regions (table 1; Fig. 3A and 3B). The Abrantes samples are from S. Miguel do Rio Torto Carbonates, characterized by dolomite and calcite marbles interbedded with mafic volcanic rocks, which have been correlated with the Lower Cambrian carbonated units of the OMZ (Moreira et al., 2015; 2016). This unit was affected by Variscan greenschist to amphibolite metamorphic recrystalization. The Assumar carbonates are included in a Detrital-Carbonated Complex, also attributed to Lower Cambrian (Pereira and Silva, 2001).

The XRD analyses (table 2) reveals a variable carbonate content in carbonates in these marbles, with three samples containing more than 95% of carbonates (GQAB-3, GQAB-7, ASS-1), three ranges between 95-80% (GQAB-4, GQAB-13, GQAB-27) and one between 80-60% (GQAB-37). Two samples are calcite marbles (GQAB-3 and GQAB-4), while the others are dolomitic (the sample GQAB-27 has a small proportion of calcite). The non-carbonate fraction in mainly composed of quartz and micas, although in some samples clay minerals (GQAB-13, GQAB-27, GQAB-37), orthose (GQAB-37) and titanite (GQAB-4) are identified. In the Assumar sample (ASS-1), the presence of chlorite is also substantial.

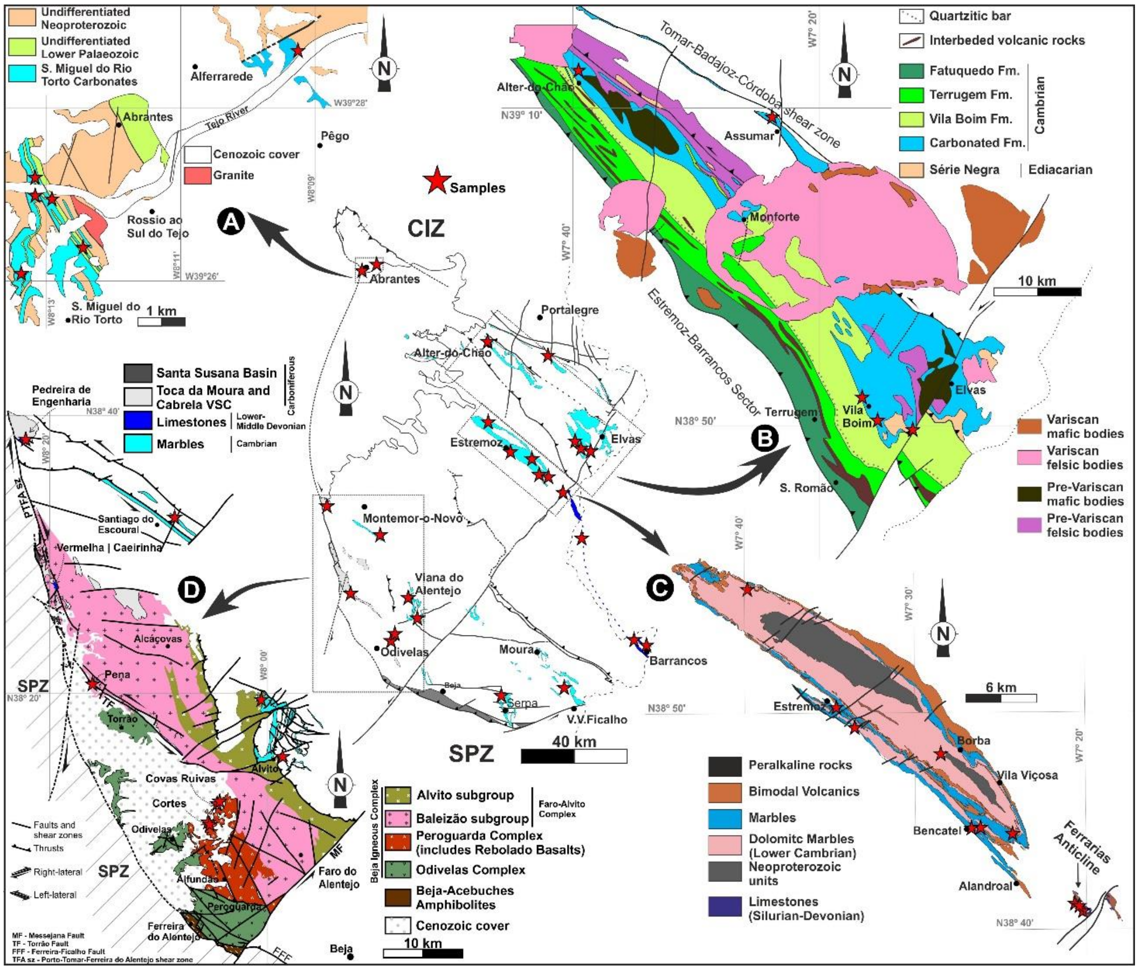

Figure 3 – Geological context of the OMZ carbonate samples:

A – Abrantes region geological map (adapted from Moreira, 2012);

B – Alter-do-Chão-Elvas sector geological map, also showing the location of the Assumar sample location (adapted from LNEG, 2010);

C – Estremoz Anticline (adapted from Piçarra, 2000; LNEG, 2010);

D – Southwest sectors of OMZ (adapted from LNEG, 2010; Moreira and Machado, in press).

The macroscopic and conventional petrographic characterization shows four distinct lithofacies of Northern OMZ carbonates (table 1):

- Samples GQAB-3 and GQAB-4 are extremely pure calcite marbles (calcite ~90%), presenting granoblastic inequigranular textures (calcite with millimetre dimensions). The non-carbonated component is mostly composed of significant quartz (5-10%) and opaque minerals.
- Sample GQAB-27 is a dolomite marble (dolomite > 80%; Fig. 4A) with granoblastic inequigranular texture, with dolomite from millimetre to submillimetre dimension. The dolomite predates metamorphism (possibly diagenetic), presenting type II (and IV?) twins (Passchier and Trouw, 2005), which shows metamorphic recrystallization of dolomite. Significant quartz (~10%) and muscovite (5-10%) and few opaque minerals compose the non-carbonated content.
- Samples ASS-1 and GQAB-7 are dolomite marbles (dolomite > 85%), with substantial quartz content (~10%). Some vestigial opaque minerals, micas (biotite or muscovite) and epidote are also identified. Two generations of dolomite are clear identified: one previous to metamorphism, with recrystallization evidences (type II twins in crystal), and a second one characterized by fine-grained turbid/cloudy dolomite (sometimes euhedral and zoned), being associated to dissolution and growing over the previous dolomite generation. The macroscopic evidences of dissolution and late dolomite precipitation was removed during sample preparation.
- Samples GQAB-13 and GQAB-37 are mainly dolomitic (>80%), characterized by pervasive dissolution and late dolomitization with abundant cloudy euhedral dolomite. The sample GQAB-13 preserves some earlier recrystallized dolomite with millimetre size, although the secondary late dolomitization is dominant (Fig. 5A). The non-carbonate fraction presents significative quartz content (5-10%), but also biotite, muscovite, amphibole, feldspars, chlorite and opaque minerals (~10%). The pervasive dolomitization is also visible at mesoscale.

III.1.5.2. Alter-do-Chão – Elvas Sector Limestones

In the Alter-do-Chão – Elvas sector, 4 samples are collected (table 1; Fig. 3B). The samples present very low-grade metamorphism and a fine-grain (submillimetric) texture, belonging to the Elvas Carbonated Unit (Oliveira et al., 1991; Moreira et al., 2014b). This unit is mainly composed of Ovetian-Marianian dolomite (and calcite) limestones, which are overlapped by the

Vila Boim Formation, with a Marianian-Biblian age based on trilobite, acritarchs and brachiopods faunas (Oliveira et al., 1991; Gozalo et al., 2003).

Table 1 – Main geographic, stratigraphic and macroscopic features of analysed samples.

		Stratigraphic features					Macroscopic features		
		Unit / Formation	Lithology	Age			Main carbonate	Secundary Dolomitization	Granularity
				Cambrian	Devonian	Silurian-Devonian			
GQAB-3	Abrantes	São Miguel do Rio Torto Carbonates	Marble	X			C	-	+++
GQAB-4	Abrantes	São Miguel do Rio Torto Carbonates	Marble	X			C	-	+++
GQAB-7	Abrantes	São Miguel do Rio Torto Carbonates	Dolomite marble	X			D	+	+++
GQAB-13	Abrantes	São Miguel do Rio Torto Carbonates	Dolomite marble	X			D	++	+++
GQAB-27	Abrantes	São Miguel do Rio Torto Carbonates	Dolomite marble	X			D	+	++
GQAB-37	Abrantes	São Miguel do Rio Torto Carbonates	Dolomite marble	X			D	++	++
ASS-1	Assumar	Assumar detrital-carbonated Complex	Dolomite marble	X			D	+	++
VB-2	Vila Boim	Elvas Carbonated Formation	Limestone	X			C	-	+
VB-12	Vila Boim	Elvas Carbonated Formation	Dolostone	X			D	+	+
VB-18	Vila Boim	Elvas Carbonated Formation	Limestone	X			C	-	+
ALT-1	Alter-do-Chão	Elvas Carbonated Formation	Dolostone	X			D	+	+
ETZ-2	Estremoz	Estremoz volcano-sedimentary Complex	Marble	X		X?	C	-	+++
ETZ-3	Vila Viçosa-Pardais	Estremoz volcano-sedimentary Complex	Marble	X		X?	C	-	+++
ETZ-5	Bencatel	Estremoz volcano-sedimentary Complex	Marble	X		X?	C	-	+++
ETZ-6A	Borba	Dolomitic Formation	Dolostone	X			D	++	++
ETZ-7	Estremoz	Estremoz volcano-sedimentary Complex	Marble	X		X?	C	-	+++
ETZ-9	Sousel	Dolomitic Formation	Dolomite marble	X			D	-	++
FER-1	Ferrarias	Ferrarias Limestone	Limestone			X?	C and D	++	++
FER-2	Ferrarias	Ferrarias Limestone	Dolosone			X?	D and C	++	++
FER-3	Ferrarias	Ferrarias Limestone	Limestone			X?	C	-	++
BA-3	Barrancos	Monte das Russianas Formation	Sandstone, calcite cement		X		C	-	+
BA-4	Barrancos	Barrancos Igneous Complex	Limestone			X?	C	-	+
BEN-1	Bencatel	-	Dolostone			X?	D and C	-	+
BEN-2	Bencatel	-	Limestone			X?	C	-	++
CHE-1	Cheles (SPN)	-	Marble	X			C	-	++
OD-1	Odivelas	Odivelas Limestone (Covas Ruivas)	Limestone		X		C	-	+
OD-2	Odivelas	Odivelas Limestone (Covas Ruivas)	Limestone		X		C	-	+
OD-4	Monte da Pena	Toca da Moura Complex (Pena Limestones)	Limestone		X		C	-	+
OD-5A	Odivelas	Odivelas Limestone (Cortes)	Limestone		X		C	-	++
OD-6	Odivelas	Odivelas Limestone (Cortes)	Bioclastic limestone		X		C	-	++
CAB-1	Cabrela	Cabrela Complex (Pedreira da Engenharia Limestone)	Dolostone		X		D	+	+
VIA-1	Viana do Alentejo	Viana-Alvito volcano-sedimentary Complex	Marble	X			C	-	+++
VIA-2	Viana do Alentejo	Viana-Alvito volcano-sedimentary Complex	Secondary dolostone	X			D	+++	+
ALV-1	Alvito	Viana-Alvito volcano-sedimentary Complex	Marble	X			D	++	+++
SRP-1	Serpa	Moura-Ficalho volcano-sedimentary Complex	Marble	X			D and C	-	+++
FIC-2	Ficalho	Moura-Ficalho volcano-sedimentary Complex	Limestone	X?		X?	C	-	+
ESC-1	Escoural	Monfurado Formation	Marble	X			C	+	+++

(C) Calcite (-) absente (+) fine-grained

(D) Dolomite (+) present (++) intermediate

(++) intense (+++) coarse-grained

(+++) prevasive

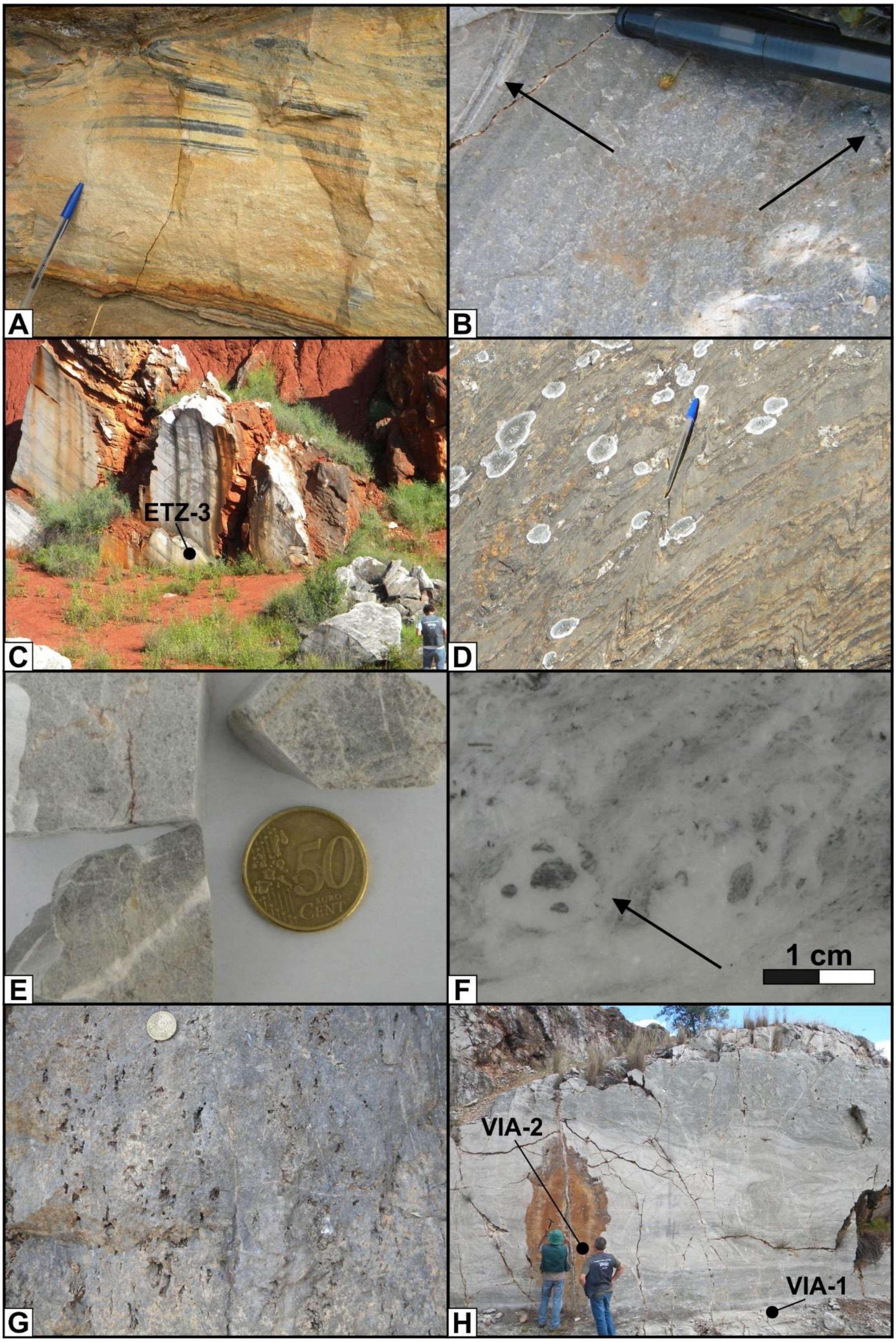

A
B
ETZ-3
C
D
50
EURO
CENT
E
1 cm
F
G
VIA-2
VIA-1
H

Figure 4 – Main macroscopic features of selected samples:

A – Dolomite marble from Abrantes sector, showing the presence of Dolomite recrystallization (AB-27 sample);

B – Fine-grained grey limestone from the Alter-do-Chão-Elvas sector, showing quartz-rich layers (VB-2 sample);

C – Sample location of the white marble from southern limb of the Estremoz anticline (ETZ-3 sample), showing the intense karstification;

D – Impure limestone from Barrancos sector (BA-4 sample). This locality provides some unclassified crinoid fragments (Piçarra and Sarmiento, 2006);

E – Macroscopic features of the Pena limestones, showing evidences of fluid interaction with late calcite veins (OD-4 sample);

F – Transverse or slightly oblique sections of (?) *cupressocrinitids* columnals from the Odivelas Limestones, typical of Middle Devonian age (OD-6 sample);

G – Macroscopic evidences of secondary late dolomitization and dissolution (CAB-1 sample);

H –Viana do Alentejo carbonates, showing the relation between VIA-1 (calcite marbles) and VIA-2 (late dolostone vein) samples.

The XRD analyses (table 2) shown that these limestones are impure, presenting more than 23% of non-carbonate mineral (Fig. 6A). Two samples (VB-2, VB-18) are calcite-rich, with a small dolomite content (lower than 1%; Fig. 6A1), and two are dolomitic (VB-12, ALT-1; Fig. 6A2). The non-carbonate fraction is composed of quartz, micas and chlorite (in one sample albite is also identified).

Petrography studies indicates two distinct lithotypes:

- Samples VB-2 and VB-18 are fine-grained impure grey calcite limestones (calcite=60-70%; Fig. 4B), with significant quartz, chlorite and epidote content (25-35%) and some sericite, amphibole, feldspars and opaque minerals (Fig. 5B). The sample VB-2 also presents some dolomite.
- Samples VB-12 and ALT-1 are fine-grained impure dolostones (dolomite=65-75%), but do not present pervasive late dolomitization at mesoscale. The dolomite is considered syn-diagenetic (or primary?) and macroscopic secondary dolomitization evidences were removed during sample preparation. Occasionally, some dissolution are recognized at thin-section scale, with generation of fine-grained cloudy late dolomite (sometimes euhedral). The first generation of dolomite sometimes presents type I twins, suggesting weak recrystallization (Passchier and Trouw, 2005). The non-carbonated content (25-30% of the sample) are mostly composed of quartz and some (chloritized) biotite, sericite, chlorite, amphibole, feldspar and opaque minerals.

III.1.5.3. Estremoz Anticline

In the Estremoz Anticline, 6 carbonates samples were collected (table 1; Fig. 3C). The Estremoz Anticline have a Neoproterozoic core, below a Cambrian sequence composed of arkosic sandstones at the base, overlapped by dolomite marbles unit (Dolomitic Formation; e.g. Oliveira et al., 1991), where the samples ETZ-6A and ETZ-9 have been collected. On top of the Dolomitic Formation, it is developed the Estremoz Volcano-Sedimentary Complex, mainly composed of calcite marbles (where the samples ETZ-2, ETZ-3, ETZ-5 and ETZ-7 have been collected) interbedded with mafic and felsic volcanic rocks (Oliveira et al., 1991). All these succession were deformed and metamorphosed under greenschist metamorphic conditions during the Variscan orogeny (Pereira et al., 2012).

The XRD analysis (table 2) indicates that the samples ETZ-2, ETZ-3, ETZ-5 and ETZ-7 are extremely pure, with a calcite content higher than 95%, while the silicate component is composed of quartz and micas (Fig. 6B). The other samples (ETZ-6A and ETZ-9) are dolomitic presenting a significant content in non-carbonate minerals (36 and 11% respectively). The non-carbonated content is mostly composed of micas and quartz, although orthose and chlorite were also identified in sample ETZ-9.

The petrographic studies identifies four distinct lithotypes:

- Samples ETZ-2 and ETZ-3 are white marbles (Fig. 4C) with no evidences of secondary dolomitization. The marbles present a granoblastic inequigranular texture. Both samples are extremely pure, being composed of calcite (>95%) and some quartz clasts. The calcite is pervasively recrystallized, showing type II twins (Fig. 5C).
- Samples ETZ-5 and ETZ-7 are dark to grey marbles, with dispersed organic matter. The marbles present granoblastic inequigranular texture, showing slightly oriented calcite crystals in ETZ-5 sample. The sample ETZ-5 is extremely pure, being mostly composed of calcite (~90%). The sample ETZ-7 is slightly more impure (calcite 80-85%), showing some layers composed of fine-grained calcite with abundant quartz (~15%) interbedded with medium-grained calcite ones. Both samples presents type I and II twins in calcite crystals, showing some recrystallization.
- Sample ETZ-6A is an impure dolostone (dolomite=60-75%), containing abundant quartz and sericite (25-30%) and some chlorite and opaque minerals. It shows clear evidences of late secondary dolomitization and dissolution from macro to microscale (Fig. 5D). The dolomite, frequently with euhedral to sub-euhedral shape, has no evidences of recrystallization, with internal zonation showing more than one episode of dolomitization (Fig. 5D).
- Sample ETZ-9 is a dolomite marble, with recrystallized dolomite crystals (~90%) and a granoblastic texture. There is no evidences of dissolution or late dolomitization, showing that the dolomite is previous to the metamorphic event (possibly diagenetic or primary?). The dolomite shows type I to type II twins, as in calcite marbles.

III.1.5.4. Bencatel-Ferrarias-Cheles-Barrancos Alignment

The presence of dolostones and limestones, spatially associated with bimodal magmatic rocks and breccias, defines the here named Bencatel-Ferrarias-Cheles-Barrancos alignment (Fig. 3; Oliveira, 1984; Araújo et al., 2013). However, the geodynamic meaning of this NW-SE to N-S alignment, which follows the general structural trend of OMZ (Fig. 3), is poorly understood. In Barrancos region (Fig. 3) these alignment was named Barrancos Igneous Complex (Araújo et al., 2013 and references therein).

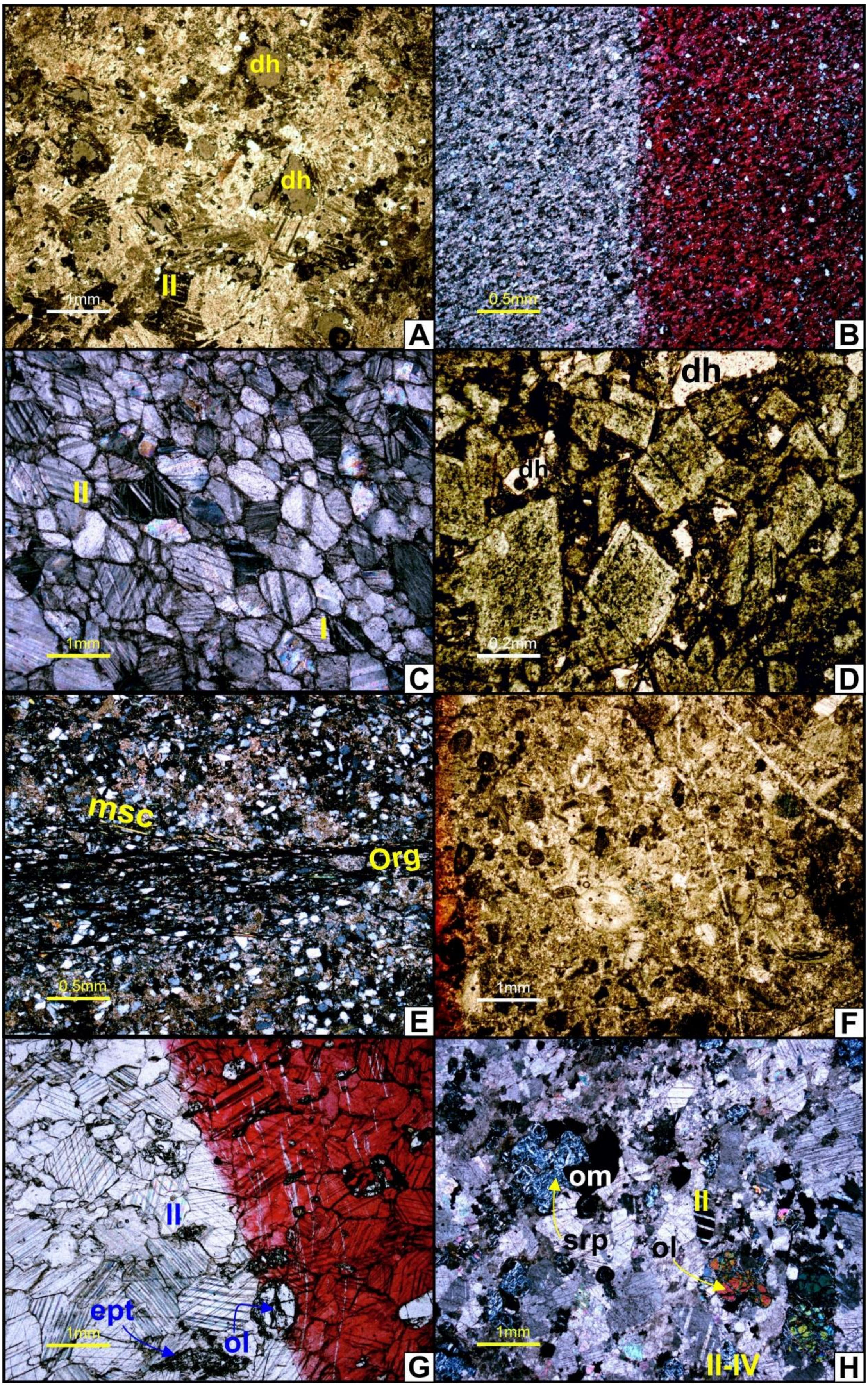

dh
dh
II
1mm
A
0.5mm
B
II
I
1mm
C
dh
dh
0.2mm
D
msc
Org
0.5mm
E
1mm
F
II
ept
ol
1mm
G
om
srp
II
ol
1mm
II-IV
H

Figure 5 – Main petrographic features of selected carbonated samples (dh – dissolution hole; msc – muscovite; org – organic matter; ept – epidote; ol – olivine; I – type I twin; II – Type II twin; IV – type IV twin; srp – serpentine; om – opaque minerals):

A – Two generations of dolomite, the first one previous to metamorphism showing recrystallized type II twins: the second one overgrowing and partially substituting the first generation (GQAB-13 sample);

B – Fine-grained calcite limestone, coloured by Alizarin Red Solution. The picture show the presence of fine-grained quartz+feldspar, muscovite and epidote (VB-18 sample);

C – Extremely pure marble from Estremoz Anticline, showing type I and II twins in calcite (ETZ-2 sample);

D – Dolostone resulting from the total substitution of primary carbonate structure, showing dissolution holes and euhedral zoned crystals of dolomite, with cloudy core and clear edges (ETZ-6A sample);

E – Sandstone with calcite cement from Monte das Russianas Formation (BA-3 sample), showing the presence of organic matter rich layers;

F – Bioclastic Devonian limestone from Odivelas Limestone (OD-1 sample);

G – Calcite marble from Viana do Alentejo, with epidote and olivine crystals in a granoblastic texture with type II twins in calcite (VIA-1 sample);

H – Serpa marble (SRP-1 sample), showing the association substitution of olivine crystal by serpentine group minerals. The carbonates are highly recrystallized with type II and IV twins.

The Barrancos and Ferrarias limestones, considered equivalent by some authors of the Estremoz Volcano-Sedimentary Complex (Piçarra, 2000), have locally Upper Silurian to Devonian fossils (Piçarra and Le Menn, 1994; Sarmiento et al., 2000; Piçarra and Sarmiento, 2006). This alignment intercepts the Cheles Limestones (Spain), considered a structural klippe structure of Lower Cambrian carbonates over the Ordovician-Silurian successions developed during the early Variscan events (Moreno and Vegas, 1976; Vegas and Moreno, 1973). The Bencatel carbonates are located in southern limb of Estremoz Anticline (Fig. 3C), presenting clear distinguish features as respect to the previously described Estremoz marbles. Seven samples are collected in this alignment (table 1): two near Bencatel (BEN-1, BEN-2), three from Ferrarias Anticline (FER-1, FER-2, FER-3), one from Cheles structure (CHE-1) and two near Barrancos (BA-3, BA-4).

The XRD analyses (table 2) indicate a strong heterogeneity in the carbonates content: more than 95% in two samples (FER-2, BEN-2), between 90 and 80% in two samples (FER-1, FER-3; Fig. 7A), between 80 and 70% in another two samples (BEN-1, CHE-1) and 57% in the last sample (BA-4). Concerning the dominant carbonate specimen: two samples are calcitic (FER-3, CHE-1), two are calcite-dominant (FER-1, BA-4), one presents similar proportion of calcite and dolomite (BEN-2), one is dolomite-dominant (BEN-1) and one is dolomitic with vestiges of calcite (FER-2). The non-carbonate content is mainly composed of quartz and micas, although some samples also present feldspars (FER-1, CHE-1) and clay minerals (BEN-1, CHE-1). The sample BA-3 presents a clearly distinct XRD pattern, with more than 80% of non-carbonated minerals (mainly composed of quartz, micas, chlorite and goethite) and the remaining 19% being composed of calcite (Fig. 7B).

The macroscopic features of samples FER-3, BA-4, BEN-1 and BEN-2 have strong similarities, being characterized by laminated dark-grey limestones, which is clearly distinct from other samples. Macro- and microscopic features allow to identify distinct lithofacies:

- Sample FER-1 have some evidences of a not pervasive late dolomitization. It is characterized by submillimetric calcite and dolomite (60%) with abundant quartz (30-35%) and some muscovite and opaque minerals. The sample contains quartz-rich layers, as well as some organic matter parallel to bedding. Some calcite veins are also identified and recrystallization are recognized. After the crushing the fragments with clear late dolomitization and late calcite veins were eliminated by visual inspection.
- Sample FER-2 is mostly composed of dolomite (70%) and abundant quartz (25%), complemented by muscovite and opaque minerals. Macro and microscale evidences of pervasive dolomitization and dissolution, with generation of euhedral cloudy late dolomite, are recognized.

- Samples FER-3 and BA-4 are impure calcite limestones (Fig. 4D) without evidences of secondary dolomitization (calcite ranges between 65 and 80%). The non-carbonated content is composed of quartz (10-30%), fine-grained muscovite (<5%), opaque minerals (~5%) and organic matter remnants. The calcite crystals presents type I twins that shows a slightly recrystallization. It is important to emphasize the presence of some hydrothermal evidences observed near the FER-3 locality.

- Samples CHE-1 is a pure calcite carbonate (~80%) with a fine-grained submillimetric granoblastic texture and no evidences of secondary dolomitization. The non-carbonated component is composed of quartz, fine-grained mica and opaque minerals and organic matter remains. The calcite shows type I twins, revealing weak recrystallization.

- Samples BEN-1 and BEN-2 are dolomite-calcite limestones (circa of 70-85%), containing abundant quartz (10-30%) and also opaque minerals and muscovite. Evidences of organic matter are clear in both samples. In samples BEN-1 dolomite seems to show some recrystallization with type I twins. Some veins of calcite are identified and it is not evident the presence of a pervasive late dolomitization at meso- and microscale.

- Sample BA-3 is a sandstone with calcite cement. The sample shows abundant quartz (60-70%), muscovite (10-15%), and opaque minerals (~5%), as well evidences of organic matter (Fig. 5E). The cement is composed of submillimetric calcite, which represents 10-15% of sample content. Although the sample was included in this sample group, it is clearly distinct, being collected in the siliciclastic Monte das Russianas Formation (Lower Devonian; Oliveira, 1984; Araujo et al., 2013).

III.1.5.5. Odivelas Limestone and Cabrela-Toca da Moura Complexes

This group includes 6 samples of Devonian grey to dark limestones *s.l.* (table I; Boogard, 1972; Machado et al., 2009; 2010; Machado and Hladil, 2010) with very low-grade metamorphism. Four samples are from Odivelas Limestones (two from Covas Ruivas locality - OD-1, OD-2 - and two from Cortes - OD-5A, OD-6) and two were collected in Toca da Moura (Pena Limestones; OD-4) and Cabrela (Pedreira da Engenharia Limestones; CAB-1) Carboniferous Basins (Fig. 3D).

The XRD analyses (table 2) emphasises the presence of the highly pure limestones, usually with carbonate content higher than 88%. One sample (CAB-1) is a dolostone, being the most impure carbonate with 11% of non-carbonate content (Fig. 7D), while the other samples are limestones, containing more than 92% of calcite (Fig. 7C). The non-carbonated content is mainly composed of quartz with some chlorite and mica.

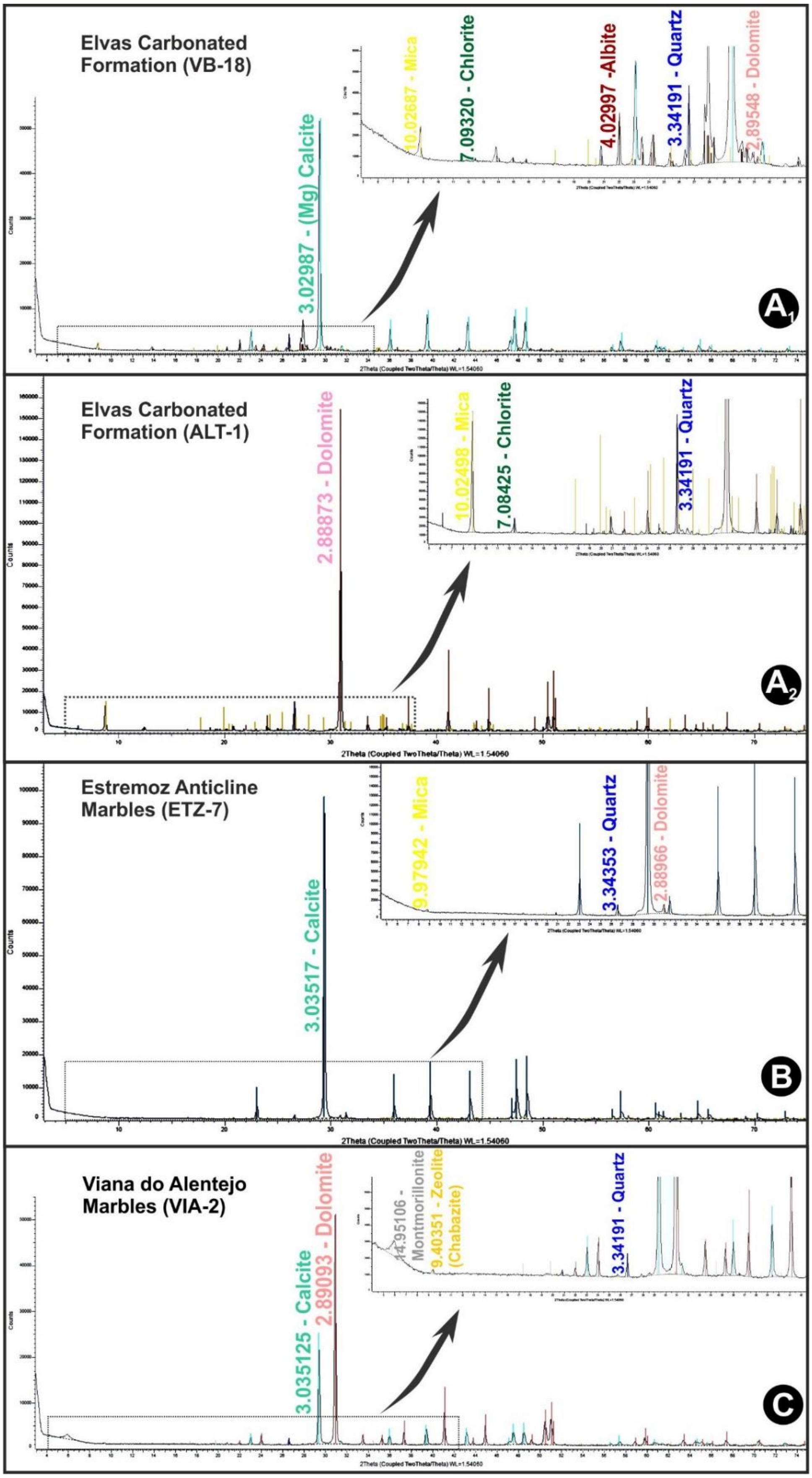

Figure 6 – XRD pattern of the Cambrian limestones (A1 and A2), the Cambrian attributed marbles (B) and a late dolostone growing in a fracture (C).

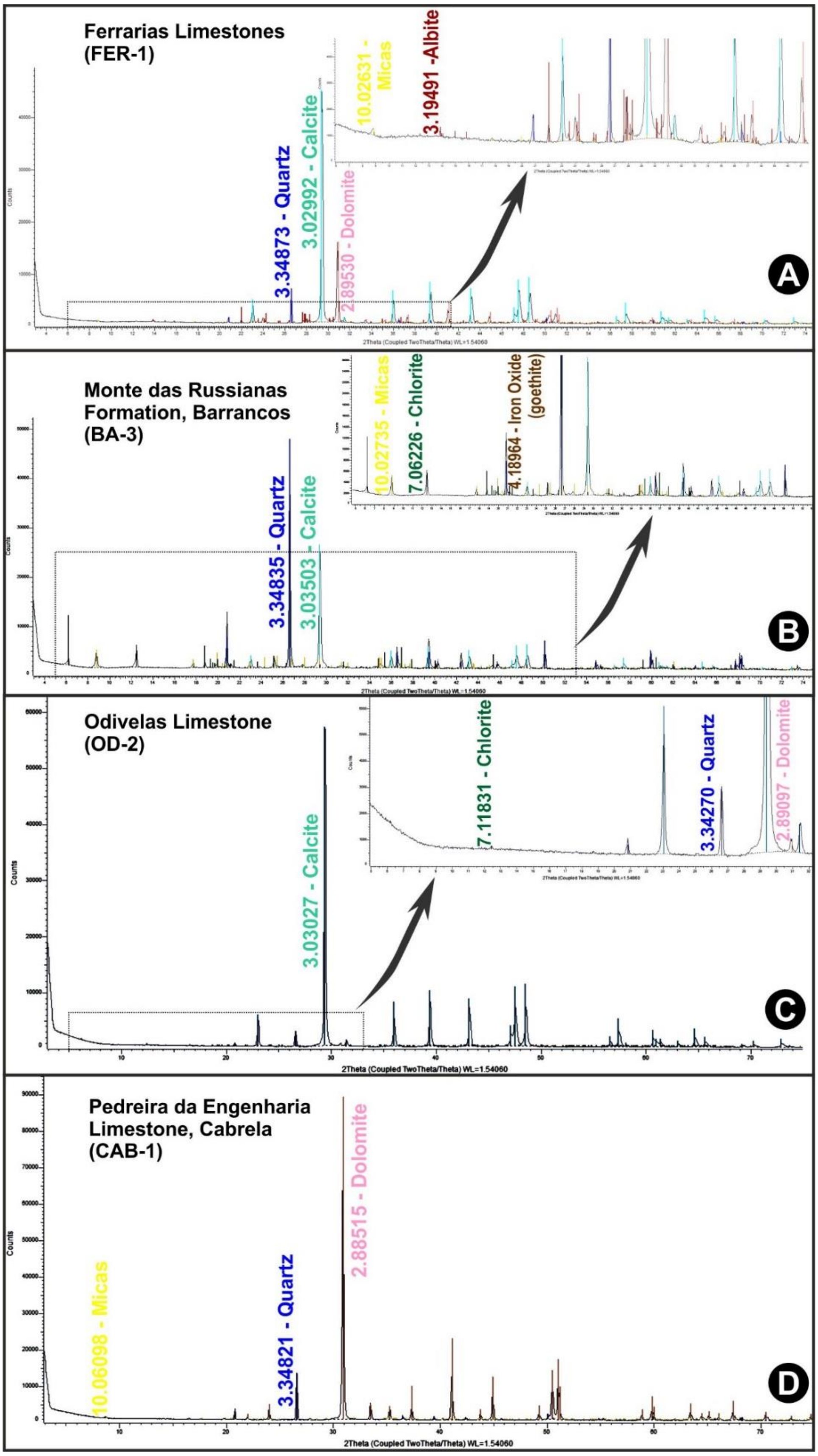

Figure 7 – XRD pattern of the Late Silurian-Early Devonian(?) limestones from Ferrarias (A), Early Devonian Sandstone with calcite cement from Barrancos (B) and Early Devonian Limestones (C) and Dolostones (D) from Odivelas and Cabrela respectively.

Table 2 – Semi quantitative results obtained by XRD analyses for the analysed samples.

	Calcite	Dolomite	Ankerite	Quartz	Mica	Chlorite	Others		obs.	Carbonates (%)	Others (%)
GQAB-3	96.17	0.00	0.00	1.42	2.42	0.00	0.00			96.17	3.83
GQAB-4	92.13	0.00	0.00	3.05	4.14	0.00	0.67	Titanite		92.13	7.87
GQAB-7	0.00	96.81	0.00	1.28	1.92	0.00	0.00			96.81	3.19
GQAB-13	0.00	94.25	0.00	1.52	0.88	0.00	3.35	Montmorillonite		94.25	5.75
GQAB-27	0.44	84.21	0.00	5.28	9.39	0.00	0.67	Kaolinite		84.65	15.35
GQAB-37	0.00	67.75	0.00	8.41	16.30	0.00	1.09 + 6.46	Kaolinite + Orthose		67.75	32.25
ASS-1	0.00	95.05	0.00	0.78	1.05	3.12	0.00			95.05	4.95
VB-2	67.74	0.23	0.00	12.31	13.93	5.79	0.00			67.97	32.03
VB-12	0.37	76.13	0.00	2.37	3.52	17.61	0.00			76.50	23.50
VB-18	74.05	0.89	0.00	5.01	14.43	0.59	5.03	Albite	Mg Calcite	74.94	25.06
ALT-1	0.00	62.06	0.00	4.16	30.80	2.98	0.00			62.06	37.94
ETZ-2	96.77	0.00	0.00	1.99	1.24	0.00	0.00			96.77	3.23
ETZ-3	95.91	0.72	0.00	0.58	2.79	0.00	0.00			96.63	3.37
ETZ-5	95.83	0.00	0.00	0.33	3.82	0.00	0.00			95.83	4.17
ETZ-6A	0.00	63.53	0.00	1.96	34.50	0.00	0.00			63.53	36.47
ETZ-7	95.52	1.22	0.00	1.07	2.19	0.00	0.00			96.74	3.26
ETZ-9	0.00	89.00	0.00	1.88	5.95	1.36	1.82	Orthose		89.00	11.00
FER-1	57.57	25.49	0.00	8.62	2.31	0.00	6.00	Albite		83.06	16.94
FER-2	0.09	95.00	0.00	2.98	1.93	0.00	0.00		Mg Calcite	95.09	4.91
FER-3	81.18	0.00	0.00	7.87	10.95	0.00	0.00			81.18	18.82
BA-3	19.25	0.00	0.00	34.70	20.07	25.35	0.63	Goethite		19.25	80.75
BA-4	55.48	1.52	0.00	15.60	27.39	0.00	0.00		Fe Dolomite	57.00	43.00
BEN-1	7.82	64.37	0.00	14.31	7.88	0.00	0.53 + 5.09	Kaolinite + Microcline		72.19	27.81
BEN-2	49.86	46.45	0.00	0.84	2.85	0.00	0.00			96.31	3.69
CHE-1	77.69	0.00	0.00	0.45	19.92	0.00	1.29 + 0.65	Kaolinite + Montmorillonite		77.69	22.31
OD-1	92.41	0.89	0.00	3.04	0.00	3.18	0.48	Hematite		93.30	6.70
OD-2	93.75	1.05	0.00	4.19	0.00	1.00	0.00			94.80	5.20
OD-4	99.53	0.00	0.00	0.47	0.00	0.00	0.00			99.53	0.47
OD-5A	96.54	0.00	0.00	0.66	0.00	0.00	2.80	Talc		96.54	3.46
OD-6	99.69	0.00	0.00	0.31	0.00	0.00	0.00			99.69	0.31
CAB-1	0.00	88.41	0.00	9.54	2.05	0.00	0.00			88.41	11.59
VIA-1	98.25	0.00	0.00	0.36	0.00	0.00	0.33 + 1.07	Titanite + Montmorillonite		98.25	1.75
VIA-2	26.02	68.95	0.00	1.48	0.00	0.00	0.63 + 2.92	Zeolite group (Chabazite) + Montmorillonite		94.97	5.03
ALV-1	8.20	0.00	82.01	0.47	0.00	9.31	0.00		or Fe Dolomite	90.21	9.79
SRP-1	8.07	88.80	0.00	0.00	0.00	1.19	1.93	Serpentine Group (Lizardite or Chrysotil)		96.87	3.13
FIC-2	64.33	0.00	0.00	31.80	3.87	0.00	0.00			64.33	35.67
ESC-1	44.90	35.56	0.00	0.13	1.15	12.00	5.52 + 0.84	Tremolite-Actinolite + Talc		80.46	19.54

The petrographic studies allow to recognize three distinct lithofacies in these limestones:

- Samples OD-1, OD-2, OD4 and OD-5A are almost composed of calcite (90-95%; Fig. 5F). Some opaque minerals and abundant organic matter were also identified. In sample OD-1 quartz is also recognized while in sample OD-5A fibrous talc is identified. The sample OD-4 has some evidences of recrystallization coupled with hydrothermal fluid interaction (Fig. 4E), while in samples OD-1, OD-2 and OD-5A, the recrystallization is less intense. Nevertheless, type I twins are present in all samples. In sample OD-1 fossil fragments were recognized (Fig. 5F).
- Sample OD-6 is a rudstone with abundant fragments of crinoids and other bioclastic material (Fig. 4F). This sample is mostly composed of calcite (>95%), some opaque minerals and frequent organic matter. The sedimentary texture presents some recrystallization with type I twins developed in the calcite.
- Sample CAB-1 is an impure dolostone (dolomite 85-90%), with frequent quartz layers. There is a secondary dolomitization associated to intense dissolution (Fig. 4G), generating a pervasive generation of cloudy euhedral dolomite, sometimes zoned, possibly replacing the initial calcite content. Some levels rich in organic matter were identified.

III.1.5.6. Southern OMZ Carbonates (Escoural, Viana-Alvito, Serpa, Ficalho)

In the southernmost sectors of the OMZ, 6 carbonate samples were collected (table 1; Fig. 3). These carbonates outcrop in antiformal structures (Araújo et al., 2013), being attributed to Cambrian based on lithostratigraphic correlation with the northern and central domains of the OMZ (Oliveira et al., 1991; Araújo et al., 2013). Two carbonated units are usually considered in this area: the basal unit composed of dolomite marbles/limestones, sometimes poorly represented (Oliveira et al., 1991), and the upper one (where all samples are collected) characterized by marbles/limestones associated with bimodal magmatism (Ribeiro et al., 1992; Oliveira et al., 1991; Araújo et al., 2013). However, in the Ficalho region, dark-grey limestones generally included in upper unit, present Silurian-Devonian conodonts (Piçarra and Sarmiento, 2006).

The XRD studies (table 2) show the presence of highly variable contents in carbonates: 2 samples with more than 95% (SRP-1 and VIA-1), 3 samples with 95-80% (VIA-2, ALV-1 and ESC-1) and one sample with significant lower values (~65%; FIC-2). The main carbonate are also heterogeneous: calcite is the only identified carbonate in VIA-1 and FIC-2 samples, while in VIA-2, SRP-1 and ESC-1, dolomite and calcite were identified, being the dolomite dominant in sample VIA-2 (Fig. 6C) and SRP-1. The sample ALV-1 also contain calcite, although the dominant carbonate is Ankerite. Concerning the non-carbonate content, quartz is present in all samples, although a greater diversity of phases is described: zeolite (VIA-2), clay minerals (VIA-1, VIA-2), chlorite (ALV-1), micas (FIC-2, ESC-1), serpentine (SRP-1), amphibole – tremolite-actinolite – and talc (ESC-1).

This group is heterogeneous, including several differential features that will be described below:

- Samples VIA-1 and VIA-2 are sampled in the same old marble quarry (Fig. 4H). The sample VIA-1 is a calcite marble (85-90%), with intense recrystalization, type II and III (and IV?) twins, and a coarse-grained (centimetric to millimetric) granoblastic texture (Fig. 5G). Olivine (forsterite?), epidote and brucite(?), but also some K-Feldspar and quartz, are recognized. The sample VIA-2 is a secondary dolostone (dolomite=60-70%) contained in a vein controlled by a fracture zone within calcite marbles. This dolostone has no evidences of recrystallization, also presenting submillimetric late calcite veins. Quartz, chlorite, opaque minerals, amphibole, feldspar and muscovite(?) compose the non-carbonated fraction. Several dissolution indications are recognized and secondary dolomite, sometimes euhedral and zoned, is pervasive.
- Sample ALV-1 is a fine-grained ankerite (85-90%) marble, with granoblastic texture, also containing quartz, chlorite, amphibole, feldspar and muscovite (?). A significant content of opaque minerals phases (iron oxides?; 2-5%) were also identified. The carbonates present type IV twins, emphasizing an intense recrystallization. Late sub-millimetric calcite veins without recrystallization were identified.
- Sample SRP-1 is mostly composed of dolomite (~70%), presenting granoblastic inequigranular (centimetric to millimetric) texture. The dolomite is considered as diagenetic (or primary?) or syn-metamorphic, showing evidences of deeply recrystallization with type II and IV twins (Fig. 5H). The non-carbonated content (20-25%) is dominated by serpentine and olivine (forsterite?), coupled with some spinel and opaque minerals (Fig. 5H). The presence of olivine relics indicates high-temperature metamorphism (Bucher and Grapes, 2011), while the serpentine is result of retrograde metamorphism. Sub-millimetric calcite (~5%), with no evidences of recrystallization, was identified, which seems to be synchronous (or later?) to the retro-metamorphism.
- Sample ESC-1 has an equigranular medium-grained granoblastic polygonal texture. It is composed of calcite and dolomite (~85%), tremolite-actinolite (5-10%), opaque minerals and talc. The carbonates show type II twins, denoting some recrystallization. There is no evidences of late dolomitization and dissolution. The tremolite should result from metamorphism under amphibolite facies conditions, while the talc could be related to the retrograde metamorphism (Bucher and Grapes, 2011).

- Sample FIC-2 is a fine-grained (submillimeric) impure limestone (calcite 65-70%), with abundant quartz (30-35%), some muscovite and dispersed organic matter. The sample do not shows evidences of late dolomitization and dissolution.

III.1.6. $^{87}Sr/^{86}Sr$ Ratio of the Carbonated Rocks

The projection of $^{87}Sr/^{86}Sr$ ratio of the OMZ carbonated rocks shows the presence of two distinct clusters (table 3; Fig. 8).

The first cluster is composed of the Odivelas and Pena limestones (OD-1, OD-2, OD-4, OD-5A, OD-6), which present $^{87}Sr/^{86}Sr$ ratio lower than 0.70800 with a very small dispersion, ranging between 0.707680 and 0.70778. However, the dolostones associated to the Cabrela Carboniferous Basin (Oliveira et al., 1991; 2013; Moreira and Machado, in press), with similar age (and genesis?), presents significant higher $^{87}Sr/^{86}Sr$ values (CAB-1; 0.70972), when compared with the Odivelas and Pena limestones (Fig. 8).

The Sr fingerprint of CAB-1 could be influenced by the interaction between the original $^{87}Sr/^{86}Sr$ ratio in limestones and the meteoric fluids (which usually have higher 87Sr/86Sr ratios; McArthur, 1994) and its "anomalous" higher value could be explained by the pervasive secondary dolomitization and dissolution (Fig. 4G). As the age of dolomitization is unknown, two hypothesis can be considered: (1) the dolomitization took place during the re-sedimentation of limestones within the intracontinental Caberla Basin (if it is considered the olistolith nature to these limestones; Oliveira et al., 2013 and references therein) or (2) the dolomitization results from recent interaction with meteoric fluids.

When comparing the Odivelas and Pena limestones it should be emphasized their similar $^{87}Sr/^{86}Sr$ fingerprint, nevertheless the presence of silicification, the oxide mineral phases and hydrothermal activity in the Pena Limestones (Machado and Hladil, 2010). Although, it must to be emphasized that only the most preserved lithofacies were analysed in Pena Limestone (OD-4 sample). This seems to indicate that, in this case, the hydrothermal interaction do not change the primary Sr ratio.

The other cluster is composed of calcite and dolomite limestones and marbles, presenting higher $^{87}Sr/^{86}Sr$ values and ranging between 0.7083 and 0.7093 (table 3). In this cluster, where there is no evidences of pervasive late dolomitization, two groups are recognized in this cluster (Fig. 8):

(1) A lower group, with ratios ranging between 0.7073 and 0.7078, is mostly composed of calcite carbonates (ETZ-2, ETZ-3, ETZ-5, ETZ-7, FIC-1, VB-2, VB-18, GQAB-3, GQAB-4) and

two dolomite carbonates affected by a pervasive metamorphic recrystallization of dolomite (ETZ-9, GQAB-27);

(2) An upper group (0.7090-0.7093) mainly composed of dolomite-rich carbonates with some evidences of late dolomitization (ALT-1, VB-12, GQAB-7 and ASS-1) and two calcite-rich marbles (VIA-1 and ESC-1), with no evidences of secondary dolomitization.

The lower group comprises Abrantes-Assumar and Estremoz marbles. Their values are similar to most of the previous published data from Estremoz marbles affected by medium grade metamorphism (Fig. 8; Marinelli et al., 2007; Taelman et al., 2013). The previous data is totally corroborant with $^{87}Sr/^{86}Sr$ ratios obtained for Alter-do-Chão – Elvas limestones (VB-2, VB-18), which have very low metamorphic grade and a well constrained age (Ovetian-Marianian; Gozalo et al., 2003). The upper group, with slightly higher ratios, contains not only the South OMZ marbles from Viana do Alentejo and Escoural (VIA-1, ESC-1; Fig. 3D), with medium to high temperature paragenesis, but also the dolomite-rich carbonates with some evidences of late dolomitization from Northern OMZ sectors (ASS-1, GQAB-7) and from Alter-do-Chão-Elvas Domain (ALT-1, VB-12).

The Serpa marble (SRP-1) presents an extremely anomalous high $^{87}Sr/^{86}Sr$ ratio (0.711052), clearly higher than the previous reported cluster, although the sample shares clear similarities with VIA-1 sample. In SRP-1 sample, the dolomite is highly recrystallized, showing that this dolomitization should be contemporaneous or previous to the metamorphic episode. Indeed, the dolomitization could be related to the interaction with hydrothermal high temperature metamorphic and/or magmatic fluids (Bucher and Grapes, 2011) during Variscan Cycle. The presence of serpentine in SRP-1 dolomite marble, resulting from retrogradation of olivine, indicates either a regional metamorphism under granulite facies or intense high temperature hydrothermal activity (Bucher and Grapes, 2011; Winter, 2013).

Thus, it could be considered that the anomalous higher values is resulted from the interaction between the high-temperature (metamorphic) fluids with Serpa Marbles, thus increasing the $^{87}Sr/^{86}Sr$ ratio. This could also explain the slightly higher values obtained to Viana do Alentejo and Escoural samples, which also presents higher metamorphic grade. Previous data from Viana do Alentejo marble had already shown higher $^{87}Sr/^{86}Sr$ values when compared with Estremoz marbles (Morbidelli et al., 2007). This possibility is in accordance with the presence of Carboniferous thermal metamorphism described in the Viana do Alentejo marbles (Gomes and Fonseca, 2006) and the presence of a high temperature event in Escoural marbles country rocks (Chichorro, 2006; Chichorro et al., 2008; Moita et al., 2009). A similar behaviour also explains the higher values obtained in Almaden de la Plata marbles (Fig. 1 and 8; Morbidelli et al., 2007), where a high temperature metamorphism is observed (Ábalos et al., 1991).

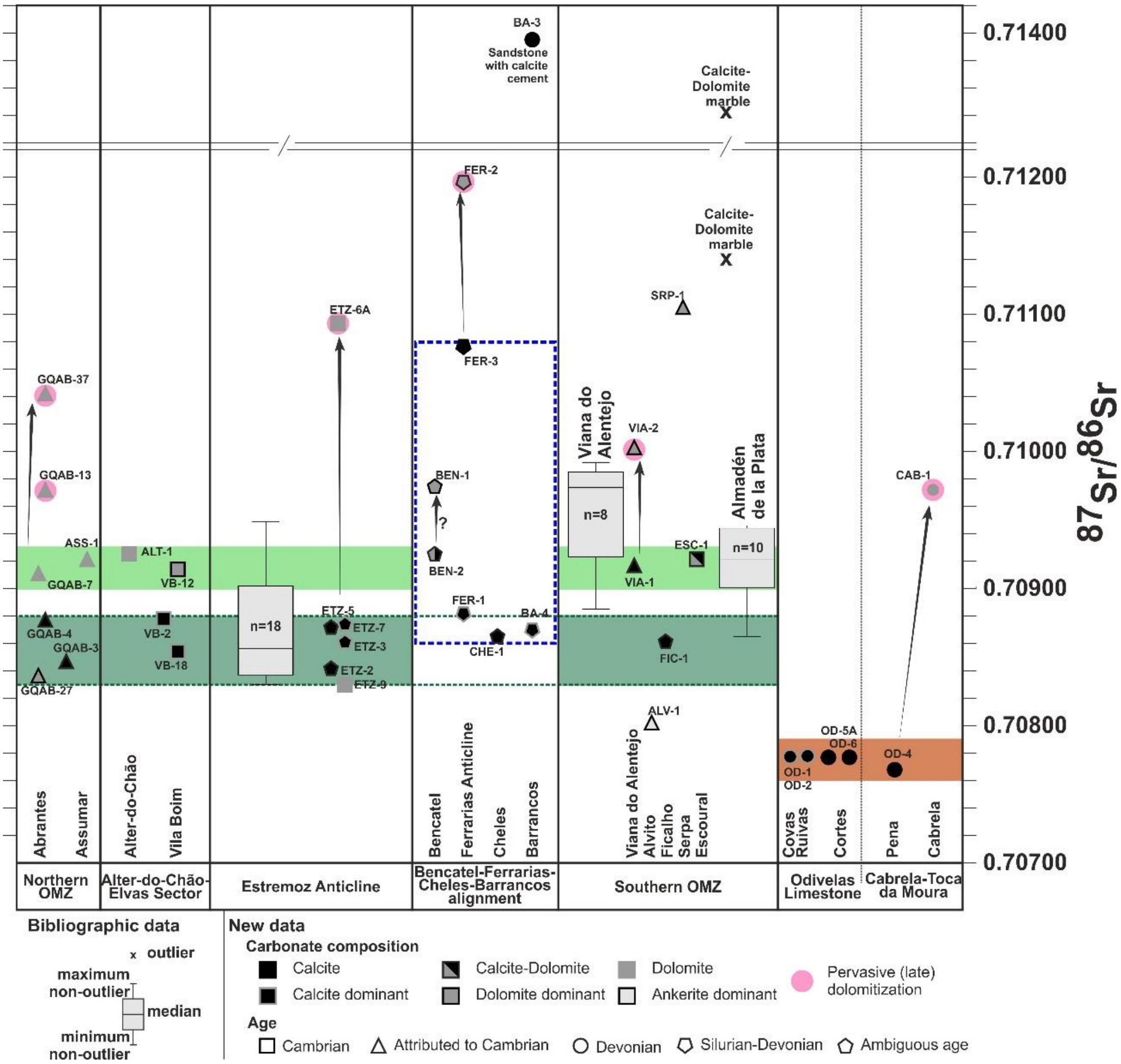

Figure 8 – Projection of $^{87}Sr/^{86}Sr$ values ratios of Palaeozoic OMZ carbonates, emphasizing the presence of different clusters (see text for more details). The arrows represents the effect of secondary/meteoric dolomitization. In the box-plots, are represented the published $^{87}Sr/^{86}Sr$ data from Viana do Alentejo, Estremoz Anticline and Almandén de la Plata marbles (adapted from Morbidelli et al., 2007; Taelman et al., 2013).

Therefore, the increase of $^{87}Sr/^{86}Sr$ values in the high-temperature metamorphic marbles (VIA-1, ESC-1 and SRP-1) is compatible with the interaction between primary $^{87}Sr/^{86}Sr$ marbles signatures and the higher $^{87}Sr/^{86}Sr$ values typical of the high temperature (metamorphic) fluids derived from upper crust (Rollinson, 1993). High $^{87}Sr/^{86}Sr$ values were obtained in OMZ Neoproterozoic-Cambrian siliciclastic rocks and in rocks resulting from anatexis of Ediacaran metasediments in the Évora Massif (Pereira et al., 2006; Moita et al., 2009). Thus, the current strontium ratio signature of these marbles (VIA-1, ESC-1 and SRP-1) could result from the mixing between primary signature and the metamorphic fluids fingerprint. This seems to show that the low to medium metamorphic grade do not change significantly the primary signature of $^{87}Sr/^{86}Sr$, contrary to what happens with high-temperature metamorphism.

The samples with pervasive secondary late dolomitization (VIA-2, ETZ-6A, GQAB-13, GQAB-37) present higher values of $^{87}Sr/^{86}Sr$, comparatively to the calcitic and dolomitic limestones/marbles without or with insipient evidences of pervasive secondary late dolomitization collected in the same sectors (Fig. 8). Similar behaviour has been reported previously to the Cabrela dolostones (Fig. 8), being interpreted as the result from the interaction between meteoric fluids and carbonated rocks.

The Alvito Fe-rich carbonate (ALV-1) despite has textural evidences of metasomatic process, shows the lowest $^{87}Sr/^{86}Sr$ value (0.708023) and is regarded as an outlier (Fig. 8). Such anomalous ratio in an ankerite-rich marble require more data in order to understand the influence of ankeritic or dolomite Fe-rich fluids in the $^{87}Sr/^{86}Sr$ ratio during the metasomatism.

The samples from Bencatel-Ferrarias-Cheles-Barrancos alignment are analysed separately because its behaviour is slightly random. Indeed, the $^{87}Sr/^{86}Sr$ data for the limestones and dolostones collected in this alignment are clearly distinct from the data for the Odivelas-Pena limestones cluster (Fig. 8). These carbonates usually presents $^{87}Sr/^{86}Sr$ values similar to those obtained in the limestones/marbles from the second cluster, ranging between 0.70860 and 0.71200, however, as mentioned the data dispersion is higher (Fig. 8):

- Samples from Cheles (CHE-1), Barrancos (BA-4) and one from Ferrarias (FER-1) presents clear similarities with the primary limestone signature of second cluster (0.708655-0.708812). Although doubts remain in relation to its age, lithostratigraphic and geodynamical significance (see discussion below);
- The Bencatel samples (BEN-1, BEN-2) presents $^{87}Sr/^{86}Sr$ values compatible with the upper group of the second cluster (0.709743 and 0.709255 respectively). Both samples contain dolomite, but is debatable the temporal relation between the dolomitization and the metamorphic processes. The strontium ratio increase could reflect the effect of secondary dolomitization on a primary Sr ratio that may be similar to CHE-1, BAR-4 and FER-1. Both samples were collected in the SW limb of Estremoz Anticline, presenting dubious position in relation to Estremoz Volcano-Sedimentary Complex.
- Ferrarias samples (FER-2 and FER-3) present significant higher values of $^{87}Sr/^{86}Sr$ (0.711960 and 0.710761 respectively; Fig. 8). As mentioned, this sector is affected by intense fracturing with evidences of intense rock/fluid interaction. This may justify the high values observed in FER-3 calcite limestone. The sample FER-2 presents a pervasive secondary dolomitization, which should increase the $^{87}Sr/^{86}Sr$ ratio;

Table 3 – $^{87}Sr/^{86}Sr$ isotopic data from studied samples (results obtained in Isotopic Geology Laboratory of Aveiro University).

Sector	Sample	$^{87}Sr/^{86}Sr$	2σ
Northern OMZ Carbonates	GQAB-3	0.708471	0.000014
	GQAB-4	0.708773	0.000026
	GQAB-7	0.709106	0.000014
	GQAB-13	0.709716	0.000024
	GQAB-27	0.708366	0.000021
	GQAB-37	0.710410	0.000017
	ASS-1	0.708866	0.000024
Alter-Do-Chão – Elvas Sector Limestones	VB-2	0.708777	0.000013
	VB-12	0.709136	0.000030
	VB-18	0.708538	0.000021
	ALT-1	0.709227	0.000024
Estremoz Anticline	ETZ-2	0.708420	0.000033
	ETZ-3	0.708610	0.000033
	ETZ-5	0.708716	0.000027
	ETZ-6A	0.710933	0.000021
	ETZ-7	0.708741	0.000027
	ETZ-9	0.708299	0.000023
Bencatel-Ferrarias-Cheles-Barrancos Alignment	FER-1	0.708812	0.000013
	FER-2	0.711960	0.000016
	FER-3	0.710761	0.000018
	BA-3	0.714002	0.000021
	BA-4	0.708694	0.000018
	BEN-1	0.709743	0.000021
	BEN-2	0.709255	0.000031
	CHE-1	0.708655	0.000021
Odivelas Limestone and Cabrela-Toca da Moura Complexes	OD-1	0.707775	0.000020
	OD-2	0.707784	0.000016
	OD-4	0.707680	0.000023
	OD-5A	0.707774	0.000017
	OD-6	0.707772	0.000016
	CAB-1	0.709720	0.000020
Southern OMZ Carbonates	VIA-1	0.709169	0.000023
	VIA-2	0.710030	0.000021
	ALV-1	0.708023	0.000025
	SRP-1	0.711052	0.000020
	FIC-2	0.708617	0.000018
	ESC-1	0.709016	0.000014

- The BA-3 sample displays the most anomalous higher $^{87}Sr/^{86}Sr$ value (0.714002; Fig. 8). This sandstone with calcite cement is composed of significant amounts of siliciclastic components. The obtained ratio should be the result either from the interaction between the silicate and carbonate components during the diagenetic process or from the interaction rock/fluid dominated by crustal fluids (Rollinson, 1993), not representative of strontium isotopic signature of seawater during the limestone precipitation.

III.1.7. $^{87}Sr/^{86}Sr$ and the age of OMZ Carbonated Episodes; a Discussion

The variation of $^{87}Sr/^{86}Sr$ ratio during the Phanerozoic times is generally well constrained (Fig. 2; McArthur et al., 2012). This could be used to have discuss or even constrain of the possible ages of the OMZ carbonated episodes.

However, the Cambrian worldwide curve of the $^{87}Sr/^{86}Sr$ values is not well constrained, due to the lack of precise biostratigraphic age of world Cambrian successions, coupled with the scarcity of well-preserved material that could be used for strontium studies (McArthur et al., 2012). Thus, several curves were proposed (Fig. 9A; Derry et al., 1994, Brasier et al., 1996, Nicholas, 1996 and Denison et al., 1998).

The Ovetian-Marianian Alter-do-Chão-Elvas limestones (Oliveira et al., 1991), with no evidences of late dolomitization, present a $^{87}Sr/^{86}Sr$ (VB-2 and VB-8; 0.708538 and 0.708777) with a very good correlation with most of the proposed worldwide seawaters values for this age (Fig. 9A; Derry et al., 1994; Brasier et al., 1996; Nicholas, 1996). Similar Sr ratio values (0.7083-0.7088) were obtained for the Ficalho limestone (FIC-2) and to the dolomite and calcite marbles from Estremoz (ETZ-2, ETZ-3, ETZ-5, ETZ-7, ETZ-9) and Abrantes (GQAB-3, GQAB-4, GQAB-27), which also have no secondary dolomitization although present an higher metamorphic-grade (greenschists to amphibolite). Such similarities support the attribution of these formations to the Ovetian-Marianian (Oliveira et al., 1991; Moreira et al., 2015; 2016), although some care should be used because similar strontium ratios are also found in some Silurian and Devonian periods (Fig. 9B and 9C).

Some Abrantes-Assumar (GQAB-7, ASS-1), Alter-do-Chão-Elvas (ALT-1, VB-12) and Southern OMZ (VIA-1, ESC-1) samples, also attributed to the same Cambrian carbonate event (Oliveira et al., 1991; Pereira and Silva, 2001; Moreira et al., 2015; 2016), present slightly higher $^{87}Sr/^{86}Sr$ values (0.7090-0.7093), that should represent the balance between the primary Sr signature with the higher strontium values provided by:

(1) The high temperature metamorphic fluids in the Viana do Alentejo and Escoural marbles;

(2) The meteoric fluids in the Abrantes-Assumar and Alter-do-Chão-Elvas carbonates.

Although it could be considered that the higher values of this sample group are compatible with the Cambrian $^{87}Sr/^{86}Sr$ worldwide curve proposed by Denison et al. (1998), we didn't support this hypothesis, which led all the other samples with lower ratios unexplained.

However, doubts still remain in Bencatel-Ferrarias-Cheles-Barrancos alignment and consequently its relation with Estremoz marbles stay debatable. Indeed, although some of these samples have $^{87}Sr/^{86}Sr$ ratios similar to those obtained to Cambrian and Cambrian attributed carbonates, they have a more complex geodynamic significance:

- The Ferrarias samples (FER-1, FER-3) are from the localities whre crinoids fragments and conodonts are found in dark limestones (Piçarra and Le Meen, 1994; Piçarra and Sarmiento, 2006), being sometimes slightly recrystallized. Locally these limestones present conglomeratic features and some limestone boulders are also found in clastic sequence. Although sample FER-3 have no evidences of dolomitization, it exhibit an anomalous higher $^{87}Sr/^{86}Sr$ values, clear dissimilar from the one of FER-1 sample. Near the FER-3 location, evidences of hydrothermal processes were identified, which could explain this value. The FER-1 $^{87}Sr/^{86}Sr$ signature is similar to those obtained in some Estremoz dark marbles (ETZ-5 and ETZ-7).

- The Bencatel samples (BEN-1 and BEN-2) are also dark calcite-dolomite limestones, collected near the fossiliferous locality of Piçarra and Sarmiento (2006). The samples are located in the southern limb of Estremoz anticline, being locally associated to some conglomeratic features. The $^{87}Sr/^{86}Sr$ values are slightly higher than Estremoz marbles.

- The Cheles sample (CHE-1) is from an isolate calcite limestone outcrop interpreted as a a klippe structure considered as Cambrian, but with no biostratigraphic data (Moreno and Vegas, 1976; Vegas and Moreno, 1973). The strontium ratios are similar to the Estremoz dark marbles.

- The Barrancos sample (BA-4) was been collected where unclassified crinoid fragments were described (Piçarra and Sarmiento, 2006), being spatially associated to breccias and bimodal volcanic rocks. Its strontium ratio is similar to the Estremoz dark marbles values.

The presence of crinoids in localities where some of the samples were collected implies, at least, an Ordovician age for these limestones (Guensburg and Sprinkle, 2001; Ausich et al., 2015), which is compatible with the considered Late Silurian to Early Devonian age based in their conodonts content (Piçarra and Sarmiento, 2006). The possible Upper Silurian age raises the possibility of correlation with Pridoli Scyphocrinites Limestone from Valle and Cerrón del Hornillo (Spain; Robardet and Gutiérrez-Marco, 2004), although this carbonate episode has not been described in Portugal (e.g. Piçarra, 2000; Piçarra and Sarmiento, 2006). The Pridoli $^{87}Sr/^{86}Sr$ signatures ranges between 0.70865 and 0.70885 (Fig. 9B; Azmy et al., 1999; McArthur et al., 2012), being concordant not only with some of the samples contained in this alignment (BA-4, FER-1 and CHE-1), but also with the dark marbles from the southern limb of Estremoz anticline (ETZ-5 and ETZ-7). In fact, the Estremoz dark marbles present a slightly higher values than the Estremoz white marbles (ETZ-2 and ETZ-3), thus being totally compatible with the strontium ratio Pridoli values. To clarify the possible existence of two distinct episodes fact it will be necessary a wider sampling in black limestones and marbles from Estremoz and Bencatel-Ferrarias-Cheles-Barrancos alignment.

The strontium ratio of the Cheles sample (0.708655) fits within the group range defined by the samples attributed to Cambrian (0.7083 and 0.7088; Fig. 9A). Nevertheless, the absence of bio- and lithostratigraphic control in these limestones prevnt a definitive conclusion.

Thus the geodynamic meaning of this alignment is still poorly known and it is possible that the two carbonate episodes are represented. In fact, the presence of carbonates associated with breccias and magmatic rocks involved by a siliciclastic matrix could indicate the presence of a syn-orogenic deposit contained boulders (olistoliths) of magmatic and carbonated rocks, with different provenances and ages.

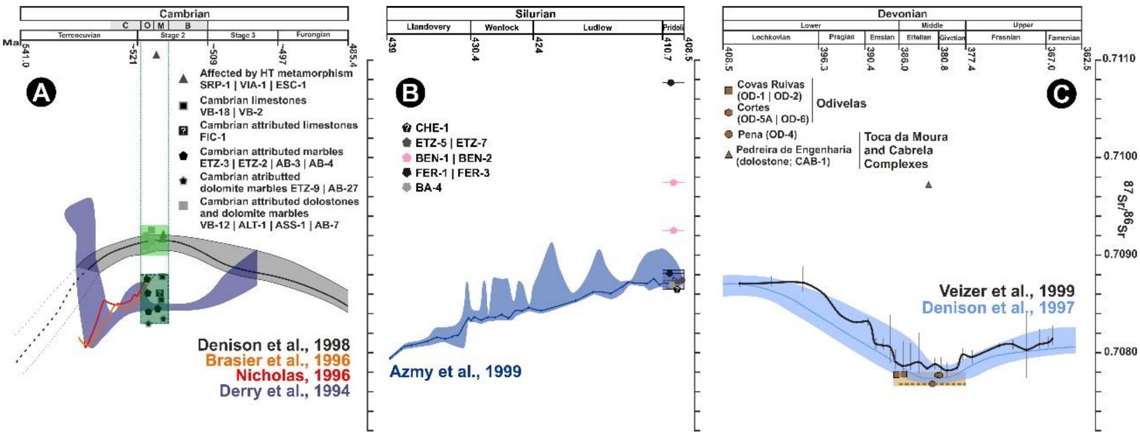

Figure 9 – Projection of OMZ data in the proposed $^{87}Sr/^{86}Sr$ curves for worldwide seawater during:

A – Cambrian (C – Corduban; O – Ovetian M – Marianian, B – Bilbilian; seawater curves adapted from Derry et al., 1994, Brasier et al., 1996, Nicholas, 1996 and Denison et al., 1998);

B – Silurian (seawater curve adapted from Azmy et al., 1999);

C – Devonian (seawater curves adapted from Denison et al., 1997 and Veizer et al., 1999).

Finally, the $^{87}Sr/^{86}Sr$ signatures of Lower-Middle Devonian Limestones not only have a very low dispertion, ranging between 0.70770 and 0.70780, but are also totally concordant with the lower $^{87}Sr/^{86}Sr$ values proposed for the worldwide seawater trend from this age (Fig. 9C; Denison et al., 1997 and Veizer et al., 1999), which is totally distinct from Cambrian and Silurian ones. Concerning the Odivelas limestones (Cortes and Covas Ruivas localities; Fig. 9C), the obtained values, ranging between 0.707784 and 0.707772, could also be explained by the interaction between the seawater and the host volcanic rocks ($^{87}Sr/^{86}Sr$ ranges between 0.7038 and 0.7066; Santos et al., 2013). However, in Pena Limestones (OD-4 sample), although the host volcanic rocks have not been identified (Moreira and Machado, in press), the isotopic ratio values remain similar (0.707680), which seems to show that such values represent the primary strontium signature of the seawater. The strong accuracy observed in all the Lower-Middle Devonian limestones also indicates that the Bencatel-Ferrarias-Cheles-Barrancos alignment limestones should not be Emsian-Givetian in age.

III.1.8. Final Remarks

This work helps to highlight some constrains in the use of $^{87}Sr/^{86}Sr$ ratios as a method to correlate the carbonated sedimentation in sedimentary and metamorphic lithostratigraphic successions.

One of the major limitations is their use in rocks with intense dolomitization related to meteoric fluids, because such process increases the $^{87}Sr/^{86}Sr$ values, due the interaction with upper crustal fluids characterized by higher strontium ratios. A similar behaviour is also expected in carbonated rocks that have interacted with high temperature metamorphic and/or hydrothermal fluids.

Nevertheless its limitation, the $^{87}Sr/^{86}Sr$ data clearly emphasize at least two events of carbonate sedimentation in the OMZ: the Lower-Middle Devonian carbonates have lower values (0.70770-0.70780), than the ratios observed in Cambrian carbonates and, perhaps, also some Silurian limestones. The Devonian data are totally corroborant with global values obtained to Emsian-Givetian worldwide Sr curve (Veizer et al., 1999).

However, the available $^{87}Sr/^{86}Sr$ ratio available are still insufficient to constrain the age and origin of the Bencatel-Ferrarias-Cheles-Barrancos carbonates and its relation with Estremoz marbles. Indeed, although the Cambrian limestones from Alter-do-Chão-Elvas (Ovetian-Marianian in age) have $^{87}Sr/^{86}Sr$ signatures similar to those obtained to Abrantes and Estremoz marbles, they are also similar to some Upper Silurian-Lower Devonian limestones from Bencatel-Ferrarias-Cheles-Barrancos alignment.

Concerning the carbonates with a possible Cambrian and Silurian ages, they present some $^{87}Sr/^{86}Sr$ ratios overlap. Thus, more studies are needed in Estremoz and Ferrarias anticlines and in Barrancos, which also should include the Scyphocrinites Limestones (Pridoli; Robardet and Gutiérrez-Marco, 2004), in order to define their distinctive $^{87}Sr/^{86}Sr$ ratio. Nevertheless, it is clear that these limestones are not from the Lower-Middle Devonian times.

The strontium studies of the OMZ carbonates prove to be adequate to the Lower-Middle Devonian and Cambrian rocks, nevertheless some doubts still remain regarding the age and origin of the from Bencatel-Ferrarias-Cheles-Barrancos carbonates and its relation with Estremoz marbles. Thus, this methodology is suitable to other OMZ carbonates without biostratigraphic data, but could also be useful in the Silurian and Ordovician marine limestones with biostratigraphic control, helping to characterize and correlate the different carbonates events based on their $^{87}Sr/^{86}Sr$ fingerprint.

References

Ábalos, B., Ibarguchi, G., Eguiluz, L. (1991). Structural and metamorphic evolution of the Almaden de la Plata Core (Seville, Spain) in relation to syn-metamorphic shear between the Ossa-Morena and South Portuguese zones of the Iberian Variscan fold belt. Tectonophysics, 191, 365-387. DOI: 10.1016/0040-1951(91)90068-4

Álvaro, J.J., Bellido, F., Gasquet, D., Pereira, M.F., Quesada, C., Sánchez-García, T., (2014). Diachronism in the late Neoproterozoic–Cambrian arc-rift transition of North Gondwana: A comparison of Morocco and the Iberian Ossa-Morena Zone. Journal of African Earth Sciences. DOI: 10.1016/j.jafrearsci.2014.03.024

Araújo, A., Piçarra de Almeida, J., Borrego, J., Pedro, J., Oliveira, J.T. (2013). As regiões central e sul da Zona de Ossa-Morena, In: Dias, R., Araújo, A., Terrinha, P., Kullberg, J.C. (Eds.), Geologia de Portugal (Vol. I), Escolar Editora, Lisboa, 509-549.

Armendáriz, M. (2006). Los depósitos carbonatados de la cuenca carbonífera del Guadiato (Córdoba, SO del Macizo Ibérico). Boletín Geológico y Minero, 117, 513-518

Ausich, W.I., Kammer, T.W., Rhenberg, E.C., Wright, D.F. (2015). Early phylogeny of crinoids within the pelmatozoan clade. Palaeontology, 58, 937-952. DOI: 10.1111/pala.12204

Azmy, K., Veizer, J., Wenzal, B., Bassett, M., Cooper, P. (1999). Silurian strontium isotope stratigraphy. Geological Society of America Bulletin, 111, 475-483. DOI: 10.1130/0016-7606(1999)111<0475:SSIS>2.3.CO;2

Boogard, M. (1972). Conodont faunas from Portugal and Southwestern Spain. Part 1: A Middle Devonian fauna from near Montemor-o-Novo. Scripta Geologica, 13, 1-11.

Boogard, M. (1983). Conodont faunas from Portugal and southwestern Spain. Part 7. A Frasnian conodont fauna near the Estação de Cabrela (Portugal). Scripta Geologica, 69, 1-17.

Brasier, M.D., Shields, G.A., Kuleshov, V.N., Zhegallo, E.A. (1996). Integrated chemo- and biostratigraphic calibration of early animal evolution: Neoproterozoic-early Cambrian of southwest Mongolia. Geological Magazine, 133, 445-485. DOI: 10.1017/S0016756800007603

Bucher, K., Grapes, M. (2011). Petrogenesis of Metamorphic Rocks. Springer-Verlag, 8th Edition, 428 p.

Burke W. H., Denison, R. E., Hetherington, E. A., Koepnick, R. B., Nelson, H. F., Otto, J. B. (1982): Variation of seawater $^{87}Sr/^{86}Sr$ throughout Phanerozoic time. Geology, 10, 516-519. DOI: 10.1130/0091-7613(1982) 10<516:VOSSTP>2.0.CO;2

Chichorro, M. (2006). Estrutura do Sudoeste da Zona de Ossa-Morena: Área de Santiago de Escoural – Cabrela (Zona de Cisalhamento de Montemor-o-Novo, Maciço de Évora). Unpublished PhD thesis, Universidade de Évora, Portugal, 502p.

Chichorro, M., Pereira, M.F., Diaz-Azpiroz, M., Williams, I.S., Fernandez, C., Pin, C., Silva, J.B., (2008). Cambrian ensialic rift-related magmatism in the Ossa-Morena Zone (Évora-Aracena metamorphic belt, SW Iberian Massif): Sm–Nd isotopes and SHRIMP zircon U–Th–Pb geochronology. Tectonophysics, 461, 91–113. DOI: 1016/j.tecto.2008.01.008

Coelho, A., Gonçalves, F. (1970): Rocha hiperalcalina de Estremoz. Bol. Soc. Geol. Portugal, XVII, 181-185.

Conde, L.N., Andrade, A.A.S. (1974). Sur la faune meso et/ou néodévonienne des calcaires du Monte das Cortes, Odivelas (Massif de Beja). Memórias e Notícias, Univ. Coimbra, 78, 141-146.

Denison, R.E., Koepnick, R.B., Burke, W.H., Hetherington, E.A., Fletcher, A. (1997). Construction of the Silurian and Devonian seawater $^{87}Sr/^{86}Sr$ curve. Chemical Geology, 140, 109-121. DOI: 10.1016/S0009-2541(97)00014-4

Denison, R.E., Koepnick, R.B., Burke, W.H., Hetherington, E.A. (1998). Construction of the Cambrian and Ordovician seawater $^{87}Sr/^{86}Sr$ curve. Chemical Geology, 152, 325-340. DOI: 10.1016/S0009-2541(98)00119-3

Derry, L.A., Brasier, M.D., Corfield, R.M., Rozanov, A.Y., Zhuravlev, A.Y. (1994). Sr and C isotope in Lower Cambrian carbonates from the Siberian craton: A paleoenvironmental record during the ‘Cambrian explosion’. Earth and Planetary Science Letters, 128, 671-681. DOI: 10.1016/0012-821X(94)90178-3

Guensburg T.E, Sprinkle, J. (2001). Earliest crinoids: New evidence for the origin of the dominant Paleozoic echinoderms. Geology 29(2): 131–134. DOI: 10.1130/0091-7613(2001)029<0131:ECNEFT>2.0.CO;2

Gomes, E.M.C., Fonseca, P.E. (2006). Eventos metamórfico/metassomáticos tardi-variscos na região de Alvito (Alentejo, sul de Portugal). Cadernos Lab. Xeolóxico de Laxe, 31, 67 - 85.

Gonçalves, F. (1972). Geological Map of Portugal, scale 1:50 000, 36-B (Estremoz), Serviços Geológicos de Portugal, Lisboa.

Gozalo, R., Liñán, E., Palacios, T., Gámez-Vintaned, J.A., Mayoral, E. (2003). The Cambrian of the Iberian Peninsula: an overview. Geologica Acta, 1, 103–112.

Hubbard C. R., Snyder, R.L. (1988). RIR-Measurement and Use in Quantitative XRD, Powder Diffraction, 3(2), 74-77. DOI: 10.1017/S0885715600013257

Hubbard, C. R., Evans, E. H., Smith, D. K. (1976). The Reference Intensity Ratio, I/Ic, for Computer simulated Powder Patterns. J. Appl. Cryst., 9, 169-174. DOI: 10.1107/S0021889876010807

LNEG (2010). Geological map of Portugal at 1:1.000.000, 3rd edition, Laboratório Nacional de Energia e Geologia, Lisboa.

Machado, G., Hladil, J. (2010). On the age and significance of the limestone localities included in the Toca da Moura volcano-sedimentary Complex: preliminary results. In: Santos A, Mayoral E, Melendez G, Silva CMD, Cachão M (Ed), III Congresso Iberico de Paleontologia / XXVI Jornadas de la Sociedad Espanola de Paleontologia, Lisbon, Portugal. Publicaciones del Seminario de Paleontologia de Zaragoza (PSPZ), 9, 153-156.

Machado, G., Hladil, J., Koptikova, L., Fonseca, P., Rocha, F.T., Galle, A. (2009). The Odivelas Limestone: Evidence for a Middle Devonian reef system in western Ossa-Morena Zone. Geol Carpath, 60(2), 121-137. DOI: 10.2478/v10096-009-0008-1

Machado, G., Hladil, J., Koptikova, L., Slavik, L., Moreira, N., Fonseca, M., Fonseca, P. (2010). An Emsian-Eifelian Carbonate-Volcaniclastic Sequence and the possible Record of the basal choteč event in western Ossa-Morena Zone, Portugal (Odivelas Limestone). Geol Belg, 13, 431-446.

Maloof, A.C., Porter, S.M., Moore, J.L., Dudás, F.O., Bowring, S.A., Higgins, J.A., Fike, D.A., Eddy, M.P. (2010). The earliest Cambrian record of animals and ocean geochemical change. GSA Bulletin, 122 (11-12), 1731–1774. doi: 10.1130/B30346.1

McArthur, J.M. (1994). Recent trends in strontium isotope stratigraphy. Terra Nova, 6, 331-358. DOI: 10.1111/j.1365-3121.1994.tb00507.x

McArthur, J.M., Howarth, R.J., Shields, G.A. (2012). Strontium Isotope Stratigraphy. In: Gradstein F.M., Ogg J.G., Schmotz M.D., Ogg G.M. (Eds.), A Geologic Time Scale 2012 (Chapter 7), Elsevier, 127-144

Medina-Varea, P., Sarmiento, G.N., Rodríguez, S., Cózar, P. (2005). Early Serpukhovian conodonts from the Guadiato Area (Córdoba, Spain). Coloquios de Paleontología, 55, 21-50.

Moita, P., Santos, J.F., Pereira, M.F. (2009). Layered granitoids: interaction between continental crust recycling processes and mantle-derived magmatism. Examples from the Évora Massif (Ossa-Morena Zone, southwest Iberia, Portugal). Lithos, 111(3–4), 125–141. DOI: 10.1016/j.lithos.2009.02.009

Morbidelli, P., Tucci, P., Imperatori, C., Polvorinos, A., Preite Martinez, M., Azzaro, E., Hernandez, M. J. (2007). Roman quarries of the Iberian peninsula: “Anasol” and “Anasol”-type. Eur. J. Mineral, 19, 125–135. DOI: 10.1127/0935-1221/2007/0019-0125

Moreira, N. (2012). Caracterização estrutural da zona de cisalhamento Tomar-Badajoz-Córdova no sector de Abrantes. Unpublished MsC thesis, University of Évora, 225 p.

Moreira, N., Machado, G. (in press). Devonian sedimentation in Western Ossa-Morena Zone and its geodynamic significance. In Quesada. C., Oliveira, J.T. (Eds.), The Geology of Iberia: a geodynamic approach. Springer (Berlin), Regional Geology Review series.

Moreira, N., Machado, G., Fonseca, P.E., Silva, J.C., Jorge, R.C.G.S., Mata, J. (2010). The Odivelas Palaeozoic volcano-sedimentary sequence: Implications for the geology of the Ossa-Morena Southwestern border. Comunicações Geológicas, 97, 129-146

Moreira, N., Araújo, A., Pedro, J.C., Dias, R. (2014a). Evolução geodinâmica da Zona de Ossa-Morena no contexto do SW Ibérico durante o Ciclo Varisco. Comunicações Geológicas 101(I), 275-278.

Moreira, N., Dias, R., Pedro, J.C., Araújo, A. (2014b). Interferência de fases de deformação Varisca na estrutura de Torre de Cabedal; sector de Alter-do-Chão – Elvas na Zona de Ossa-Morena. Comunicações Geológicas, 101(I), 279-282.

Moreira, N., Pedro, J., Romão, J., Dias, R., Araújo, A., Ribeiro A. (2015). The Neoproterozoic-Cambrian transition in Abrantes Region (Central Portugal); Litostratigraphic correlation with Cambrian Series of Ossa-Morena Zone. The Variscan belt: correlations and plate dinamics. Géologie de la France (Variscan 2015 special issue, Rennes), 2015(1), 101-102. ISBN: 978-2-7159-2612-7.

Moreira, N., Pedro, J., Santos, J.F., Araújo, A., Romão, J., Dias, R., Ribeiro, A., Ribeiro, S., Mirão, J. (2016). $^{87}Sr/^{86}Sr$ ratios discrimination applied to the main Paleozoic carbonate sedimentation in Ossa-Morena Zone. In: IX Congreso Geológico de España (special volume). Geo-Temas, 16(1), 161-164. ISSN 1576-5172.

Moreno, F., Vegas, R. (1976). Tectónica de las séries ordovícias y siluricas en la región de Villanueva del Fresno. Estudios geológicos, 32, 47-52.

Nicholas, C.J. (1996). The Sr isotopic evolution of the oceans during the 'Cambrian explosion'. Journal of the Geological Society, 153, 243-254. DOI: 10.1144/gsjgs.153.2.0243

Oliveira, J.T. (1984). Transversal Barrancos-Ficalho. Cadernos do Laboratorio Xeolóxico de Laxe, 8, 347-357

Oliveira, J.T., Relvas, J., Pereira, Z., Munhá, J., Matos, J., Barriga, F., Rosa, C. (2013). O Complexo Vulcano-Sedimentar de Toca da Moura-Cabrela (Zona de Ossa Morena): evolução tectono-estratigráfica e mineralizações associadas. In: Dias, R., Araújo, A., Terrinha, P., Kullberg, J.C. (Eds.), Geologia de Portugal (Vol. I), Escolar Editora, Lisboa, 621-645.

Oliveira, J.T., Oliveira, V., Piçarra, J.M. (1991). Traços gerais da evolução tectono-estratigráfica da Zona de Ossa Morena, em Portugal: síntese crítica do estado actual dos conhecimentos. Comun. Serv. Geol. Port. 77, 3-26.

Palácios Gonzalez, M.J. Palacios, T., Valenzuela, J.M.G (1990). Trilobites y Goniatites de la cuenca carbonífera de los Santos de Maimona: deducciones bioestratigráficas. Geogaceta, 8, 66-67.

Passchier, C.W., Trouw, R.A.J. (2005). Microtectonics. 2nd Edition, Springer, 382P..

Pereira. Z., Oliveira, J.T. (2003). Estudo palinostratigráfico do sinclinal da Estação de Cabrela. Implicações tectonostratigráficas. Cienc. Terra UNL Lisboa, 5, 118–119.

Pereira, Z., Oliveira, V., Oliveira, J.T. (2006). Palynostratigraphy of the Toca da Moura and Cabrela Complexes, Ossa Morena Zone, Portugal. Geodynamic implications. Rev Palaeobot Palyno, 139, 227-240. DOI: 10.1016/j.revpalbo.2005.07.008

Pereira, M.F., Silva, J.B. (2001). The Northeast Alentejo Neoproterozoic-Lower Cambrian succession (Portugal): implications for regional correlations in the Ossa morena Zone (Iberian Massif). Geogaceta, 30, 106-111.

Pereira, M.F., Medina, J., Chichorro, M., Linnemann, U. (2006). Preliminary Rb-Sr and Sm-Nd isotope geochemistry on Ediacaran and Early Cambrian Sediments from the Ossa-Morena Zone (Portugal). In: J. Mirão & A. Balbino (Eds.), VII Congresso Nacional de Geologia abstract book (vol. I), Estremoz, 213–215.

Pereira, M.F., Solá, A.R., Chichorro, M., Lopes, L., Gerdes, A., Silva, J.B. (2012). North-Gondwana assembly, break up and paleogeography: U–Pb isotope evidence from detrital and igneous zircons of Ediacaran and Cambrian rocks of SW Iberia. Gondwana Research, 22(3-4), 866-881. DOI: 1016/j.gr.2012.02.010

Piçarra, J.M. (2000). Estudo estratigráfico do sector de Estremoz-Barrancos, Zona de Ossa Morena, Portugal. Vol. I - Litoestratigrafia do intervalo Câmbrico médio?-Devónico inferior, Vol. II - Bioestratigrafia do intervalo Ordovícico-Devónico inferior. PhD Thesis (unpublished), Évora University, Portugal.

Piçarra, J.M., Le Meen, J. (1994). Ocorrência de crinóides em mármores do Complexo Vulcano-Sedimentar Carbonatado de Estremoz: implicações estratigráficas. Comunicações do Instituto Geológico e Mineiro, 80, 15-25.

Piçarra, J.M., Sarmiento, G. (2006). Problemas de posicionamento estratigráfico dos Calcários Paleozóicos da Zona de Ossa Morena (Portugal). In: J. Mirão & A. Balbino (Eds.), VII Congresso Nacional de Geologia abstract book (vol. II), Estremoz, 657-660.

Prokoph, A., Shields, G.A., Veizer, J. (2008). Compilation and time-series analysis of a marine carbonate $\delta^{18}O$, $\delta^{13}C$, $^{87}Sr/^{86}Sr$ and $\delta^{34}S$ database through Earth history. Earth-Science Reviews, 87, 113-133. DOI: 10.1016/j.earscirev.2007.12.003

Ribeiro, M.L., Mata, J., Piçarra, J.M. (1992). Vulcanismo bimodal da região de Ficalho: características geoquímicas. Comunicações Serviços Geológicos de Portugal, 78(2), 75-85.

Robardet, M., Gutiérrez-Marco, J.C. (1990). Passive margin phase (Ordovician-Silurian-Devonian). In: Dallmeyer RD, Martínez García E (Ed), Pre-Mesozoic geology of Iberia, Springer-Verlag, Berlin, 249-251.

Robardet, M., Gutiérrez-Marco, J.C. (2004). The Ordovician, Silurian and Devonian sedimentary rocks of the Ossa-Morena Zone (SW Iberian Peninsula, Spain). J Iber Geol, 30, 73-92

Rollinson, H.R. (1993). Using geochemical data: evaluation, presentation, interpretation, Addison-Wesley Longman Ltd, Singapore, 352p.

Romão, J., Ribeiro, A., Munhá, J., Ribeiro, L. (2010). Basement nappes on the NE boundary the Ossa-Morena Zone (SW Iberian Variscides). European Geosciences Union, General Assembly, Vienna, Austria (Abstract).

Sánchez-García, T., Quesada, C., Bellido, F., Dunning, G.R., González de Tánago, J. (2008). Two-step magma flooding of the upper crust during rifting: the Early Palaeozoic of the Ossa Morena Zone (SW Iberia). Tectonophysics, 461, 72–90. DOI: 10.1016/j.tecto.2008.03.006

Sánchez-García, T., Bellido, F., Pereira, M.F., Chichorro, M., Quesada, C., Pin, C., Silva, J.B. (2010). Rift-related volcanism predating the birth of the Rheic Ocean (Ossa-Morena zone, SW Iberia). Gondwana Research, 17, 392-407. DOI: 10.1016/j.gr.2009.10.005

Santos, J.F., Andrade, A., Munhá, J. (1990). Magmatismo orogénico varisco no limite meridional da Zona de Ossa-Morena. Comun. Serv. Geol. Portugal, 76, 91-124.

Santos, J.F., Mata, J., Ribeiro, S., Fernandes, J., Silva, J. (2013). Sr and Nd isotope data for arc-related (meta) volcanics (SW Iberia), Goldschmidt Conference Abstracts, 2132.

Sarmiento, G.N., Piçarra, J.M., Oliveira, J.T. (2000). Conodontes do Silúrico (Superior?)-Devónico nos “Mármores de Estremoz”, Sector de Estremoz-Barrancos (Zona de Ossa Morena, Portugal). Implicações estratigráficas e estruturais a nível regional. I Congresso Ibérico de Paleontologia/VIII International Meeting of IGCP 421 (abstract book), Évora, 284-285.

Sarmiento, G.N., Gutiérrez-Marco, J.C., Del Moral, B. (2008). Conodontos de la "Caliza de Pelmatozoos" (Ordovícico Superior), Norte de Sevilla, Zona de Ossa-Morena (España). Coloquios de Paleontología, 58, 73-99.

Sarmiento, G.N., Gutiérrez-Marco, J.C., Rodríguez-Cañero, R., Martín Algarra, A., Navas-Parejo, P. (2011). A Brief Summary of Ordovician Conodont Faunas from the Iberian Peninsula. In: Gutiérrez-Marco, J.C., Rábano, I. and García-Bellido, D. (eds.), Ordovician of the World. Cuadernos del Museo Geominero, IGME, 14, 505-514. ISBN 978-84-7840-857-3

Silva, J.C., Mata, J., Moreira, N., Fonseca, P.E., Jorge, R.C.G.S., Machado, G. (2011). Evidence for a Lower Devonian subduction zone in the southeastern boundary of the Ossa-Morena-Zone. In: Absctracts of the VIII Congresso Ibérico de Geoquímica, Castelo Branco, 295-299.

Taelman, D., Elburg, M., Smet, I., Paepe, P., Lopes, L., Vanhaecke, F., Vermeulen, F. (2013). Roman marble from Lusitania: petrographic and geochemical characterization. Journal of Archaeological Science, 40, 2227-2236. DOI: 10.1016/j.jas.2012.12.030

Vegas, R., Moreno, R. (1973). Sobre la tectónica del flanco meridional de la Antiforma de Burgillos (sur de la provincia de Badajoz). Estudios Geologicos, 29, 513-517.

Veizer, J., Ala, D., Azmy, K., Bruckschen, P., Buhl, D., Bruhn, F., Carden, G.A.F., Diener, A., Ebneth, S., Godderis, Y., Jasper, T., Korte, C., Pawellek, F., Podlaha, O.G., Strauss, H. (1999). $^{87}Sr/^{86}Sr$, δ13C and δ18O evolution of Phanerozoic seawater. Chemical Geology, 161, 59-88. DOI: 10.1016/S0009-2541(99)00081-9

Veizer, J. (1989). Strontium Isotopes in Seawater through Time. Ann. Rev. Earth Planet. Sci., 17, 141-167. DOI: 10.1146/annurev.earth.17.1.141

Vera, J.A., (Eds., 2004). Geología de España. SGE and IGME, 884p.

Winter, J.D. (2013). Principles of igneous and metamorphic petrology. 2nd edition, Pearson New International Edition. ISBN13: 9781292021539